ABSTRACT

WANG, GONGBO. Sindbis Virus Interaction with Cells. (Under the direction of Dennis T. Brown)

Sindbis virus is the prototype of *Togaviridae* family, *Alphavirus* genus. In nature, alphaviruses can infect and grow in both mammals and insects. They can also reproduce themselves in many laboratory cell cultures. Understanding the virus infection process is fundamental for drug discovery and vaccine development. Two scenarios of alphavirus infection have been proposed. One proposed mechanism involves uptake of virion into endocytic vesicles followed by low-pH dependent fusion and genome release. This infection pathway was first discovered in influenza and proposed later to be the entry mechanism for most enveloped viruses. The other mechanism proposes direct penetration at the cell surface and neutral pH, supported by both electron microscopy and biochemical studies. We studied the ability of Sindbis virus to infect Baby Hamster Kidney (BHK) in the absence of endocytosis. Instead of using drugs or cellular mutations, we used low temperature to inhibit endocytosis. We performed an antibody escape experiment at different temperatures combined with a plaque assay. Our results showed that Sindbis virus can infect cells in the absence of endocytosis at both 5 and 15 ^{o}C. To confirm these results, we infected BHK cells at low temperatures with Sindbis virus containing Green Fluorescent Protein (GFP) gene as a reporter. The result shows that Sindbis virus is capable of injecting its genome into host cell and initiating an infection under conditions which have been established to inhibit endocytosis and membrane fusion.

Sindbis virus has a host derived membrane bilayer. E1 and E2 are the two structural proteins that are anchored in this membrane by their transmembrane (TM) domains. Studies on chimeric alphavirus composed of Ross River E1 and Sindbis E2 proteins revealed a role of E1-E2 TM domain interaction in affecting virus stability (Strauss, Lenches, and Strauss, 2002). The importance and characteristics of different amino acids in E2 TM domain was also studied by making deletions in the region (Hernandez et al., 2003; Whitehurst et al., 2006). We studied the impacts of making deletions in E1 TM domain on virus life cycle. Although short deletions at different positions result in diverse infectivity, virus assembly is normal for all the short deletion mutants we constructed. We also found that large deletions in E1 TM domain are lethal to virus production by severely inhibiting the virus budding process, while structural protein synthesis and nucleocapsid assembly are not impaired. We also constructed a combined double deletion mutant in which short deletions were made in both E1 and E2 TM domains. The combined double deletion mutant produced no infectious viruses. These results provided important information about E1-E2 TM domain interaction.

Sindbis Virus Interaction with Cells

by
Gongbo Wang

A dissertation submitted to the Graduate Faculty of
North Carolina State University
in partial fulfillment of the
requirements for the Degree of
Doctor of Philosophy

Biochemistry

Raleigh, North Carolina

2008

APPROVED BY:

Dr. Dennis T. Brown Chair of Advisory Committee	Dr. Keith Weninger Vice Chair of Advisory Committee
Dr. Paul Wollenzien	Dr. E. Stuart Maxwell
Dr. Jason A. Osborne Minor Representative	

DEDICATION

谨以此博士论文献给我远在中国的父亲王怀波和母亲公维芝。这篇总结我二十一年受教育历程的博士论文中，只有在这短短的一页里我可以使用母语来表达我感恩的心情。我的双亲用他们所能承担的一切来养育我、教育我、激励我、支持我走到今天。这篇论文以及我即将获得的博士学位不仅仅是我一个人的成就，而是我们全家人的。我所能在此提及的支言片语并无法示及父母养育大恩的万分之一。

To my parents, Wang, Huaibo and Gong, Weizhi. This is the only page I can express myself in my native language throughout this Ph.D. thesis that concludes my 21-year education. My parents, who have raised me, educated me, inspired me and supported me all my life, contributed everything they could afford to lead me towards this grand achievement. This thesis and the degree I will receive is not only my own achievement, but my family's. All I can describe in this short page is not even comparable to a tiny bit of what my parents have devoted for me.

BIOGRAPHY

I was born Wang, Gongbo in Shenyang, China on November 11th, 1980 to Wang, Huaibo and Gong, Weizhi. As the only offspring of my parents, I have no siblings but seven cousins. My father is the Chief Accountant of the biggest securities company in Shenyang. My mother works for an international company where she is the Chairman of the Employees' Union.

My education life started in 1987 when I went to Qinggonger Elementary School in the Tiexi District of Shenyang. After passing ridiculous numbers of exams in 1993, I was admitted into Northeast Yucai Middle School where I finished both middle school and high school education. In the year of 1999, I was admitted into School of Life Sciences, Fudan University located in Shanghai, China. Without many surprises, I graduated in four years from college with a bachelor's degree. Then I came to North Carolina State University located in the City of Raleigh, State of North Carolina in U.S.A. seeking a higher degree. Things went really well. And I will get my Ph.D. in the August of 2008 at the age of 27.

Being the first Chinese generation born after the "Culture Revolution" and "Mao era", my personal life verifies the prosperity of China and her economic growth. At the time I was born, both my parents were labor workers, who did not get the chance of higher education because of the Culture Revolution. They earned only enough money not to starve. Fortunately, through their vigorous personal endeavors such as taking night classes, my parents found better jobs provided by the "new"

economy policy. By the time I finished elementary school, my family started having savings. My parents paid to get me started on taking advanced courses in math and English outside regular school. All of this helped me in passing the exams required to go to the best middle school in Shenyang. We also moved several times to bigger and bigger apartments, which are common accommodations for most people in big Chinese cities. Middle school and high school were fun. I was with the same classmates for six years and made a lot of life-time friends. After high school, I left my hometown. College life was hard and competitive in Fudan. In the first two years of my college life, I worked so hard that I suffered from depression. This also partially led to my breakup with a girl I grew up with. That chaotic period became the turning point of my life, as I realized for the first time in my life that there were always more important things than academic achievement and career. I also learned to cherish what I already have. For the rest of my college life, I found a perfect balance among academic achievement, health and pursuit of happiness. Other than that, I need to mention I made a lot of very good friends in college, most of whom are Shanghainese.

I came to Raleigh, North Carolina right after I graduated from college and started the American chapter of my life. Americans accepted me with warmth and generosity. There was no culture clash at all. Instead, I found that the traditional Chinese views on working and dealing with relationships work perfectly well in the American context, at least in my case. My lab mentors, Dennis T. Brown and Raquel Hernandez, are both renowned alpha-virologists. They have not only directed and

helped me in research, but also treated me as their family member. Besides in the lab, I made a lot of friends by taking courses. It is impossible to mention all of their names here. My American friends helped me get furniture, buy a car and do course work when I first arrived. They also took me into their homes to meet their families, drove me to the capitol of the country and hung out with me. It was quite an experience to make so many friends in a foreign country.

Also in North Carolina State University, I met Qiqi Wang, who shares a very common Chinese family name with me that sometimes confuses Americans. She has been my companion, best friend and family in the past four years.

I will go to the University of Texas Medical Branch at Galveston in the September of 2008 to start a post-doctoral position. I am switching gears to study pathology and immunology.

ACKNOWLEGEMENTS

Committee members: Dennis T. Brown (NC State, Biochemistry), Keith Weninger (NC State, Physics), E. Stuart Maxwell (NC State, Biochemistry), Paul Wollenzien (NC State, Biochemistry), Jason A. Osborne (NC State, Statistics).

Lab mentors: Dennis Brown (NC State, Biochemistry), Raquel Hernandez (NC State, Biochemistry)

TABLE OF CONTENTS

LIST OF FIGURES

CHAPTER 1

CHAPTER 2

CHAPTER 3

CHAPTER 4

LIST OF TABLES

CHAPTER 5

Chapter 1

Introduction to Sindbis Virus

Alphavirus and its transmission pathway

Sindbis virus was first isolated in 1952 from a pool of mosquitoes in Egypt. It is the prototype of *Togaviridae* family, *Alphavirus* genus. 25 other members of this genus have been identified. Viruses in this genus are called alphaviruses. Eastern Equine Encephalitis (EEE), Venezuelan Equine Encephalitis (VEE), Semliki Forest (SF), Chikungunya (CHIK), Ross River (RR) and Western Equine Encephalitis (WEE) are commonly seen alphaviruses (Strauss and Strauss, 1994). Alphaviruses are transmitted in nature among birds, rodents and domestic animals by blood sucking insects such as mosquitoes, ticks, midges and sand flies. Therefore they are also categorized as **ar**thropod **bo**rne **virus**es (**arbovirus**es), which include alphaviruses, flaviviruses and (-)-strand RNA bunyaviruses.

The life cycle of alphavirus involves insects, birds, mammals and humans. Rodents and birds are natural reservoirs of these viruses. Blood sucking insects carry viruses they obtain from a blood meal and infect other host animals during later bites. The transmission can be enzootic within the same animal population. Alphaviruses can also be transmitted epizootically to domestic animals and humans. Some alphaviruses may cause severe diseases in infected birds and animals leading to their deaths. After being bitten by an infected mosquito, host humans develop a febrile disease. Most alphaviruses induce potent immune response in human body which results in the elimination of virus and no severe symptoms. While some viruses, such as Chikungunya, can cause severe and prolonged symptoms in

humans. In this case, viremic humans produce sufficient virus for the mosquito vectors to transmit the disease onto other humans or animals after a blood meal.

The structure of Sindbis virion

Sindbis virus has stable structure and high yield from lab cell cultures, making it the ideal subject for studying alphavirus structure. Additionally, it is non-pathogenic in humans rendering it easier and cheaper to handle. Figure 1.1 shows the cryo-electron microscopy (cryo-EM) reconstruction image of Sindbis virion (Paredes et al., 1993). The Sindbis virion is about 70 nm in diameter. The outer surface is covered exclusively by E1 and E2 proteins, noted in yellow. E1 and E2 have 439 and 423 amino acids, respectively. Both proteins have a molecular mass of about 50 kDa. The ectodomains are glycosylated and palmitoylated post-translationally. The two glycoproteins form heterodimers, every three of which form a trimer. The white circle in Figure 1.1 outlines one trimer composed of three E1 and three E2 proteins. Each Sindbis virus has 80 of these trimers. If we draw lines between the centers of adjacent trimers, we can find pentagons (shown in green lines) and hexagons (shown in red lines). Each Sindbis virus has 12 such pentagons and 30 such hexagons in a symmetric construction. This is equivalent to T=4 icosahedral symmetry structure (Caspar and Klug, 1962; Fuller, 1987; Paredes et al., 1993; Vogel et al., 1986; von Bonsdorff and Harrison, 1975).

Figure 1.2 shows a cut-away view of Sindbis virus derived from cryo-EM reconstruction of the entire virion and the inner nucleocapsid, respectively. The blue

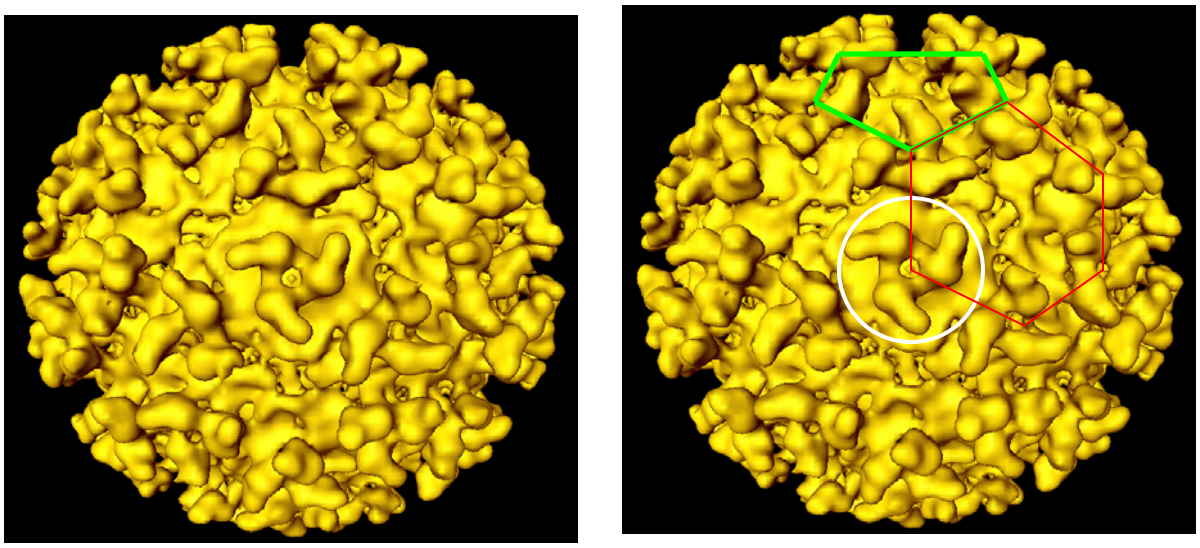

Figure 1.1: Sindbis virus outer surface from a cryo-electron microscopy reconstruction. (Paredes et al., 1993)

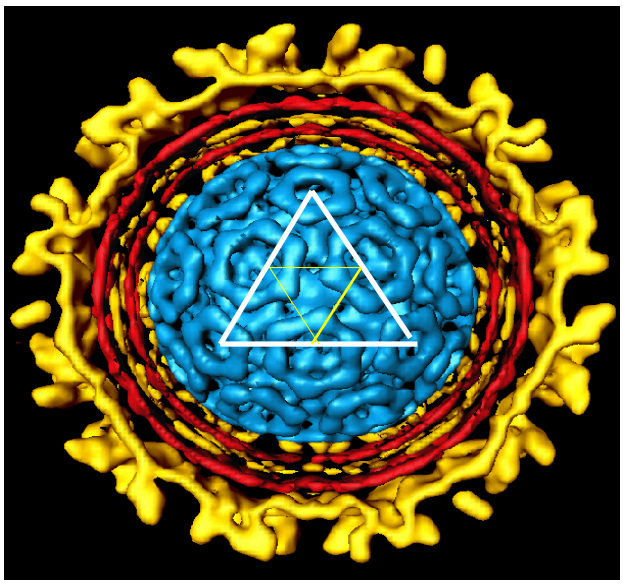

Figure 1.2: Cut-away image of Sindbis virus from cryo-electron microscopy reconstruction. (Paredes et al., 1993)

inner protein shell is composed of 240 copies of the same capsid protein, 30-kDa in size. The triangles drawn on the inner protein shell signify the traditional way of identifying T=4 icosahedral symmetry structure. The red lipid bilayer is derived from the host membrane. E1 and E2 glycoproteins have transmembrane domains that anchor them in the host derived membrane bilayer. E2 has a 33-residue cytoplasmic domain, while E1 has a short cytoplasmic domain of only 2 residues (Strauss and Strauss, 1994). The cytoplasmic domains are involved in an interaction with the capsid protein, which is important for the stability of Sindbis virus. As shown in Figures 1.1 and 1.2, the inner nucleocapsid shell has the same T=4 icosahedral symmetry as the outer glycoprotein shell. In the center of the whole structure is one plus sense, single stranded genomic RNA, which is not shown in Figure 1.2.

Sindbis viral genome

The Sindbis viral genome is composed of one RNA molecule with a 5' cap and 3' poly-A tail. The molecule is packed in the core of nucleocapsid with high density, filling the provided space. The Sindbis viral genome can be seen as two parts: the 5'-terminal two-thirds and the 3'-terminal one-third of the RNA. The 5' portion contains the genetic information of four non-structural proteins, nsP1, nsP2, nsP3 and nsP4. The non-structural proteins have methyltransferase, helicase, protease and RNA polymerase activities. The 3' part of the genome encodes a polyprotein that is processed into capsid, E2, E1 structural proteins and two small polypeptides, E3 and 6K. E1, E2 and capsid compose the main skeleton of a Sindbis

virion. Trace amount of E3 and 6K protein has been reported to be present in mature Sindbis virions. (Gaedigk-Nitschko and Schlesinger, 1990; Liljestrom et al., 1991; Lusa, Garoff, and Liljestrom, 1991)

Alphavirus infection and life cycle: attachment

It is generally believed that alphavirus infection is started by the attachment of a virion to a cell receptor, like all other viruses. The receptor of alphavirus infection is not known. Since Sindbis virus can reproduce in many laboratory cell cultures derived from different organs of both insects and mammals, the cell receptor/s must be a universal class of molecules that are presented in all of these cells. It is also possible that alphaviruses can utilize different receptors, as insect and mammalian cells differ in many aspects.

Alphavirus infection and life cycle: penetration

Following receptor attachment, alphavirus penetrates into the cell and releases its genome into the cytosol. There are two proposed mechanisms on how this process is carried out.

One proposed pathway involves endocytosis and fusion. In this scenario, virus particles are assimilated into endosomes under the mediation of cell receptors. Acidification of endosomes then triggers conformational changes in viral proteins, which mediate a fusion event between viral and endosomal membranes (Bressanelli et al., 2004; Jardetzky and Lamb, 2004). Fusion results in disassembly of virus

particle and release of the viral genome into the cytosol (Helenius, 1984; Helenius and Marsh, 1982; Marsh, 2006). This infection pathway was first found in influenza viruse and later proposed to be the entry mechanism for all enveloped viruses and some non-enveloped viruses (Marsh, 2006).

Evidence supporting the role of endocytosis in alphavirus penetration includes inhibition of virus production by cellular mutations (DeTulleo and Kirchhausen, 1998), lysosomotropic weak bases (Cassell, Edwards, and Brown, 1984; Helenius, Marsh, and White, 1982) and other drugs that raise the pH of endosomes (Marsh, Bolzau, and Helenius, 1983). The assays employed in these experiments measure viral RNA or structural protein synthesis; processes which occur after expression of the non-structural proteins, negative strand synthesis and subgenomic RNA production must have taken place. Viral RNA and structural protein synthesis are comparatively late events that require the correct functioning of the infected cell. However, drugs and mutations may have multiple effects. In other words, they may directly or indirectly impair other functions related to viral RNA and structural protein synthesis. These indirect effects were demonstrated in mosquito cells in which, it was shown that some weak bases such as chloroquine can not inhibit virus production and others interfere with virus production by blocking proteolytic processing of the non-structural precursor protein (Hernandez, Luo, and Brown, 2001).

Evidence supporting alphavirus entry by low-pH dependent fusion comes from data produced in virus-liposome model systems and the fact that alphaviruses

can induce cell-cell fusion (Bron et al., 1993; Kielian, 1995; Kielian and Jungerwirth, 1990; Lu and Kielian, 2000; White, Kartenbeck, and Helenius, 1980). The ability of alphaviruses to induce fusion between cells in a pH dependent manner was developed to support the notion that viral and cellular membranes can fuse at low pH. This fusion event was proposed to be the same as what happens between the viral and endosomal membranes when endosome acidification occurs. However, it was later shown that this fusion property is actually a two-step event (Edwards and Brown, 1986). Fusion does not occur until the pH is switched to acidic and brought back to neutral. Maximum fusion was achieved when pH went to 5.3 and came back to 7.4. No fusion occurs at pH 5.3. This is a different scheme as the one-time pH switch to acidity which occurs in endosomes. Another line of evidence supporting the role of fusion in alphavirus infection comes from observing the interaction between virus and liposomes, which are the substitute of cells in the system (Kielian, 1995; Kielian et al., 2000; Kielian and Jungerwirth, 1990). But there are several issues with this artificial system concerning the validity of replacing cells with liposomes. First of all, the liposomes used did not have cell receptors or any other protein contents. Although the cell receptor for alphavirus is unknown, it is an essential component in virus infection. Secondly, it was also shown that a high concentration of cholesterol (25%) is required in the liposome mixture for fusion to occur (Kielian and Helenius, 1984; Lu, Cassese, and Kielian, 1999). However, alphaviruses can reproduce in mosquito cells, which have only less than 3% of their total sterol as cholesterol (Hernandez, 2006; Luukkonen, Brummer-Korvenkontio, and Renkonen, 1973;

Rietveld, Koorengevel, and de Kruijff, 1995). Additionally, depending on the composition of the liposomes, fusion can occur at different pH values (Bron et al., 1993; Haywood and Boyer, 1985). By changing the proportion of lipids and cholesterol, virus can fuse with liposomes at neutral pH. Finally, when fusion between virus particles and cells in the context of pH switches was examined by electron microscopy, the two steps of the pH switch are still required (Paredes et al., 2004).

The crystal structure of alphavirus E1 protein has been deemed to support the fusion model (Gibbons et al., 2004; Jardetzky and Lamb, 2004). The crystal structure of E1 was achieved at both neutral and acidic pH. An analogy of the fusion protein in influenza virus to E1 has been proposed. However, the crystal structure of E1 was achieved using treatment with detergent, which suggests that the obtained structure may not be in its native configuration (Mulvey and Brown, 1994; Whitehurst et al., 2007). According to the crystal structures, the fusion protein of influenza virus, hemmaglutinin, undergoes a reorganization of the domains with a pH change to acidic. Although E1 protein completes a similar change according to crystal structures and molecular modeling, this change requires refolding of the protein in a manner which is hard to achieve in the native environment of an intact virus. Plus, E1 and E2 form heterodimers instead of functioning entirely independently. There is no evidence that E1 can undergo the same conformational changes found in the crystal structures when it is found as part of the native heterodimer.

A novel proposed mechanism is the direct penetration of virus at the cell surface in a pH independent manner (Paredes et al., 2004). In this scheme, the binding of virus to the cell receptor is followed by a pore formation between virus and the infected cell. This pore (Koschinski et al., 2005) is hypothesized to provide a channel through which the viral RNA is injected into the cytosol. This mechanism does not require endocytosis or fusion. Chapters 2 and 3 of this thesis will focus on this aspect of the alphavirus infection cycle. More details on data supporting this mechanism and how the whole process is proposed to occur will be provided.

Alphavirus infection and life cycle: genome replication

After the viral genome is introduced into the cells, part of the cellular machinery for translation is hijacked. Alphavirus has four non-structural proteins on the 5' end of viral genome. They are named after nsP1, nsP2, nsP3 and nsP4, according to their order in the RNA. The non-structural proteins are translated from the 5' end of full length genomic RNA as two polyproteins, nsP123 and nsP1234. There is an opal codon at nucleotide 1897 of the non-structural open reading frame between nsP3 and nsP4. When translation terminates at that opal codon, nsP123 is produced (Strauss, Rice, and Strauss, 1983). nsP123 polyprotein contains the sequence of nsP1, nsP2 and nsP3. nsP1234 polyprotein, possessing an extra nsP4 sequence, is produced when opal codon read through occurs (Fig. 1.3). As non-structural proteins are not components of a mature virion, they do not function until after virus penetration. Both polyproteins and their cleaved products are functional

during infection. Some of them may form a complex with host proteins to carry out replicase activity (Strauss and Strauss, 1994). Non-structural proteins are not as extensively studied as the structural proteins, but there is much information available. nsP1 appears to be necessary for minus-strand RNA synthesis. nsP2 has proteinase activity and is required for 26S subgenomic RNA synthesis. nsP2 may have the RNA helicase activity. The functions of nsP3 are not well defined. nsP4 seems to possess RNA polymerase activity to help with (-)-strand synthesis (Keranen and Kaariainen 1979; Sawicki, Sawicki et al. 1981; Strauss and Strauss 1994).

Following expression of these essential non-structural proteins, complementary minus strand RNA is produced. In the presence of both viral and cellular proteins that have RNA dependent RNA polymerase activity, two plus strand RNAs are made from the minus strand, the full length genomic RNA and a 26S subgenomic RNA. The subgenomic mRNA, one third of the full genome in size, is also 5' capped and 3' polyadenylated. This RNA is simply a copy of the 3' end nucleotide sequence in the full length genomic RNA. Only the full length genomic RNA is packaged into a mature virion.

Alphavirus infection and life cycle: assembly of nucleocapsid

The structural proteins are first translated as a polyprotein from the 26S subgenomic RNA, which is posttranslationally cleaved into capsid, E1, E2, E3 and 6K (Strauss and Strauss, 1994). After translation is initiated on cytoplasmic

ribosomes, the capsid protein is removed from the polyprotein by an autoproteolytic activity. The signal sequence exposed by the removal of capsid directs the insertion of a polyprotein with six transmembrane domains (Fig. 1.4) into the endoplasmic reticulum membrane (Hernandez et al., 2003) and then processed into pE2, 6K and E1 by signalase (Liljestrom and Garoff, 1991). pE2, the precursor of E2, is then cleaved into E2 and E3 proteins by furin during the transport of pE2-E1 complex. The transmembrane domain near the C-terminus of pE2 reorients into the cytoplasm during maturation (Liu and Brown 1993; Liu and Brown 1993). E1 and E2 proteins also undergo posttranslational decorations such as glycosylation and palmitoylation.

After the expression of structural polyprotein and autoproteolytic removal of capsid, assembly starts as genomic RNA is associated with a capsid protein. This complex serves as a base for nucleocapsid assembly. The encapsidation process is specific, as normally only full length RNA is packaged (Weiss et al., 1989). Nucleocapsids that are empty or contain other RNAs are not assembled. Only a single RNA molecule is packaged in the nucleocapsid, and presumably the size of the genomic RNA is at the limit of what 240 capsid proteins can encapsidate.

Alphavirus infection and life cycle: budding

Replication and encapsidation of the viral genome occurs in the cytoplasm, while E1 and E2 proteins are synthesized and transported to the plasma membrane through trans-Golgi network (Moehring et al., 1993). In mammalian cells, preassembled nucleocapsids are found distributed throughout the cytosol. A specific

interaction between the endodomain of E2 glycoprotein and capsid directs budding and maturation of virus particles (Lopez et al., 1994). Each capsid protein finds and binds to an E1-E2 heterodimer. While this pairing process occurs, virus particles bud through the plasma membrane. At the end of the process, nucleocapsid is sealed in a protein shell of E1-E2 glycoproteins. During this process, the lipids associated with the transmembrane domains of glycoproteins become part of the virus structure. The lipid bilayers finally merge and form a membrane bilayer sandwiched between the capsid and glycoprotein shells. Upon completion of this process, the mature virus can proceed to infect the next host cell and reproduce.

Transmembrane Domain Interaction between E1 and E2

The Alphavirus genome is protected by two protein shells. Between the protein shells is a host derived membrane bilayer. E1 and E2 proteins have transmembrane domains so that they can pass through the bilayer and contact the inner shell. There is evidence that E1 and E2 transmembrane domains interact with each other at the molecular level (Strauss, Lenches, and Strauss, 2002). Sequential deletions were made in the E2 transmembrane domain (Hernandez et al., 2003; Whitehurst et al., 2006). Deleting a single methionine (M379) dropped the titer by four orders of magnitude. Interestingly, the titer is restored gradually when more amino acids were deleted from the domain. Deletions in the E2 transmembrane domain do not affect the assembly process but have a dramatic impact on virus infectivity and stability. To further study the importance of the E2 transmembrane

domain, serial deletions were made that cover all faces of the helix throughout the length of the domain. The data indicate that deletions closer to the cytoplasmic face reduced virus infectivity much more than deletions closer to the luminal side of the membrane (Whitehurst et al., 2006).

In looking for E1-E2 transmembrane domain interactions, amino acids in E1 transmembrane domain were also deleted. These results including virus titer, viral protein synthesis, and virus assembly will be shown and discussed in Chapter 4.

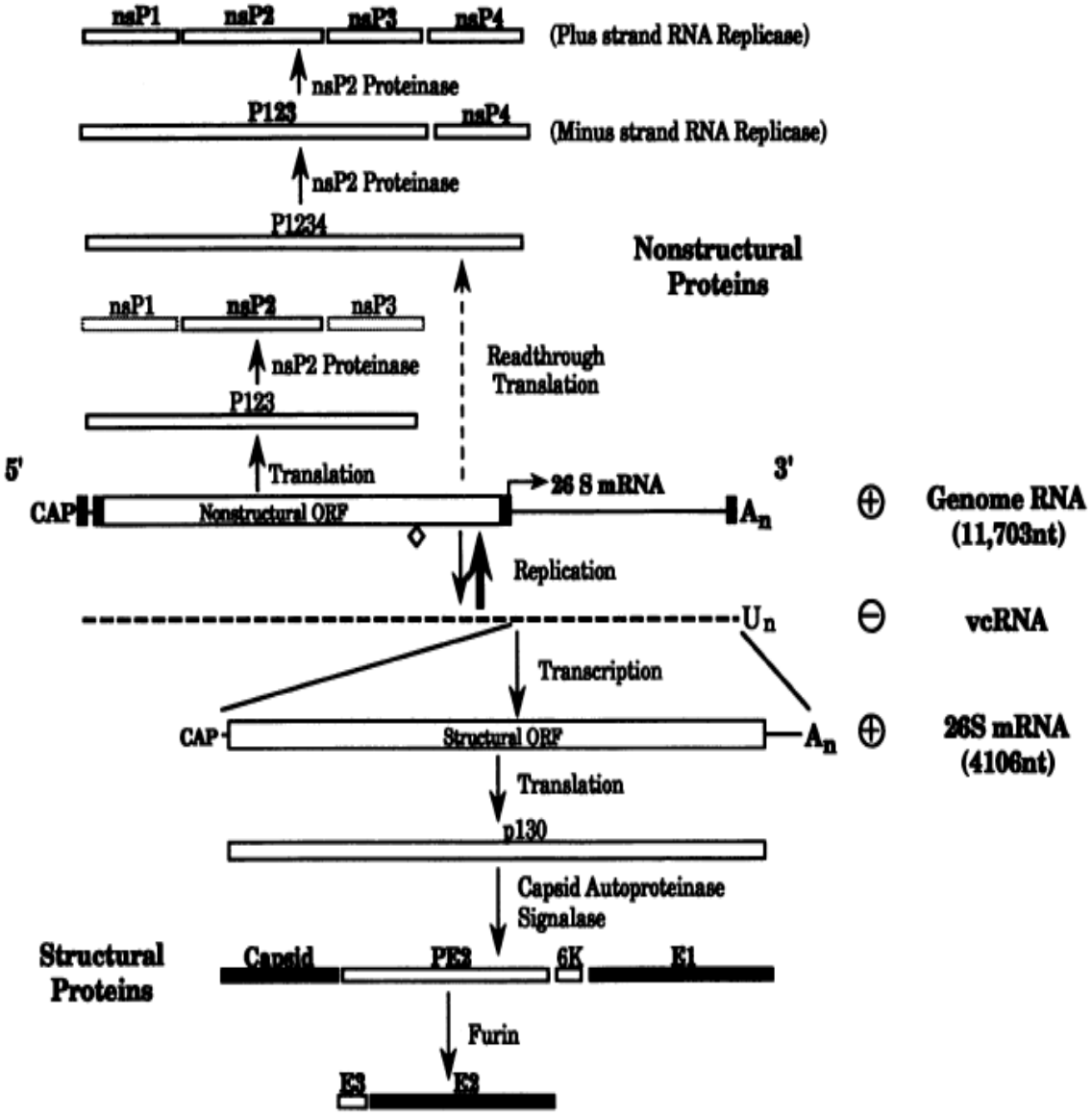

Figure 1.3: Organization, replication and expression of Sindbis virus genome. (Strauss and Strauss, 1994)

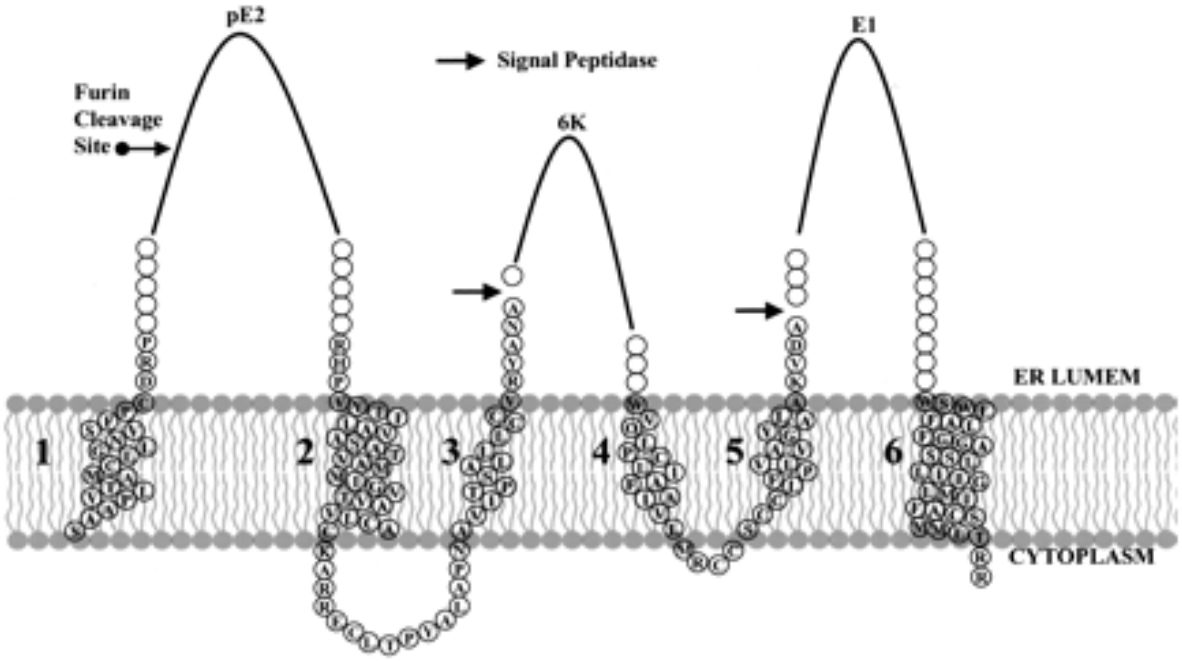

Figure 1.4: A schematic representation of Sindbis virus structural polyprotein in the ER membrane. The polyprotein is processed by signal peptidase and furin activity after integration so that 6K protein and transmembrane domain 1 are cleaved. Transmembrane domain 3 flips during the maturation process and becomes the cytoplasmic domain of the mature E2 protein. (Hernandez et al., 2003)

CHAPTER 2

Sindbis virus infection at low temperatures

Gongbo Wang, Raquel Hernandez, Keith Weninger and

Dennis Brown

Published in:

Virology. 2007 June 5; 362(2): 461-467

It is widely held that membrane containing viruses employ those membranes as tools of infection (Eckert and Kim 2001; Marsh and Helenius 2006). These enveloped viruses gain entry to potential host cells by fusing the virus membrane with the host cell membrane. This fusion event is mediated by proteins integrated into the virus membrane and serve as motors to drive the fusion process (Jardetzky and Lamb, 2004). Virus fusion proteins can mediate the process of fusion with a host cell membrane in a low pH dependent or independent manner (Marsh and Helenius, 2006). In the low pH independent pathway, it is proposed that virus glycoproteins interact with a cell receptor and that this interaction induces protein conformational changes which drive the fusion of the virus membrane with the cell membrane. An example of virus entering cells by fusion at the cell surface is HIV (Cardoso et al., 2005; Eckert and Kim, 2001). In the low pH dependent pathway it is proposed that upon interaction with a receptor, virus particles are internalized into endosomes. In the late endosome and upon acidification, pH induced conformational changes in the virus proteins lead to membrane fusion (Kielian and Jungerwirth, 1990). This latter pathway has been proposed for many families of viruses and is best demonstrated for influenza virus (Stegmann, Booy, and Wilschut, 1987). Influenza virus has been convincingly demonstrated to enter cells from the low pH environment of a late endosome (Tamm, 2003). The process of influenza virus fusion with the cell membrane has been investigated using a liposome model system (Stegmann et al., 1985). It has also been demonstrated that alpha (and flavi) viruses can fuse with protein free liposome membranes upon exposure to acidic pH

(Gibbons et al., 2004). A significant difference in the putative fusion inducing proteins of influenza virus and the alphaviruses is a dramatic dissimilarity in structure and sequence (Gibbons, Vaney et al. 2004; Modis, Ogata et al. 2004; Zaitseva, Mittal et al. 2005). Because of these differences, the proteins are referred to as Type I (Flu) and Type II (alphavirus) fusion proteins. Type I fusion proteins are found in a wide variety of unrelated virus families (Eckert and Kim, 2001). Type II fusion proteins are found only in the insect vectored Alpha and Flaviviruses. Their ability to fuse with liposomes and the observations that inhibitors of endosome acidification or mutations which block endosome formation can prevent subsequent virus RNA or protein synthesis have been presented as evidence that Alpha and Flaviviruses also penetrate cells from the acidic environment of endosomes (Helenius, Marsh et al. 1982; DeTulleo and Kirchhausen 1998). Each of these experiments has presented problems in their interpretation. Fusion with protein free liposomes has been demonstrated to “absolutely” require the presence of cholesterol in the liposome membrane (Kielian and Helenius, 1984). Liposomes employed in these studies typically contain 25-50 mole% cholesterol. Insects are the alternate host for these viruses and their membranes have less than 3% cholesterol (Rietveld et al., 1999). Insect cell lines, such as SF21 cells (Cha et al., 1997) (Gibco, Invitrogen) have been adapted to synthetic growth medium (Weiss et al., 1993) (SF900IISFM, Gibco, Invitrogen) that contains < 5% cholesterol. It has been shown that Japanese Encephalitis Virus can infect and replicate in these cells (Kim et al., 2004). We have found that Sindbis virus readily infects and passages in these cells

(to be published elsewhere). Studies using endosome acidification inhibitors or cells encoding genetic defects in the endocytic pathway measure the products of late events such as RNA or protein synthesis to determine that penetration has not taken place. These events occur several steps after penetration. These experiments raise the possibility that the defect in virus production may occur after penetration. In one instance it has been shown that a reagent blocking endosome acidification does not block penetration but rather blocks processing of virus non-structural proteins to form the RNA replicating complex (Hernandez, Luo, and Brown, 2001).

The structures of Alpha and Flaviviruses present an innate barrier to the fusion process. The Alphavirus particle is composed of two symmetrically identical T=4 icosahedral protein shells nested one inside the other (Paredes et al., 1993). The virus membrane is sandwiched between the two shells and protected by the outer shell. Intramolecular disulfide bridges are involved in the lateral associations which stabilize the outer protein shell (Anthony, Paredes et al. 1992; Mulvey and Brown 1994). The E1 protein is assembled in a lateral matrix with fenestrations at the 5 and 6 fold axes above the membrane bilayer. Disassembly of this protein lattice would be required to expose the underlying membrane bilayer and allow the fusion event to occur. We have previously shown that the process of fusion of the Sindbis virus membrane with the membrane of a living host cell is a two step process requiring exposure to acidic pH (to set up conditions for fusion) and return to neutral pH (to execute the fusion event) (Edwards and Brown 1986; Paredes, Ferreira et al. 2004). This contrasts with the process of virus fusion with artificial

liposomes which does not require a return to neutral pH and suggests that interactions with living cells are more complex in nature. In electron microscope studies we have found that when infectious Sindbis virus particles interact with the surface of living cells they lose their electron dense core. This suggests that the virus RNA has been transferred to the cell (Figure 2.1) (Paredes, Ferreira et al. 2004). These data led to the hypothesis that interaction of the virus spike glycoproteins with the cell surface resulted in the formation of a protein pore in the cell plasma membrane through which the virus RNA passed to initiate infection. Evidence supporting the formation of such a pore during virus infection has subsequently been provided (Koschinski et al., 2005). Events related to the process of penetration occurred at the cell surface in the absence of endocytosis and at neutral pH (Paredes, Ferreira et al. 2004). In these experiments we found that about 25% of particles attached to the cell surface became empty at 37 ^{o}C. To our surprise 3% of particles attached became empty if the cell monolayers were maintained at 4 ^{o}C. This number is significant because Sindbis does not assemble empty particles, the virus employed was purified 2X by density gradient centrifugation and no empty particles were seen if virus was fixed prior to addition to cells. These observations suggested that some events related to the infection process could occur at temperatures which prevent endocytosis and indeed prevent all vesicular transport (Lippincott-Schwartz, Roberts, and Hirschberg, 2000).

It is well known that at temperatures below 19 ^{o}C endocytosis in mammalian cells is arrested and at temperatures around 15 ^{o}C all cellular vesicular transport is

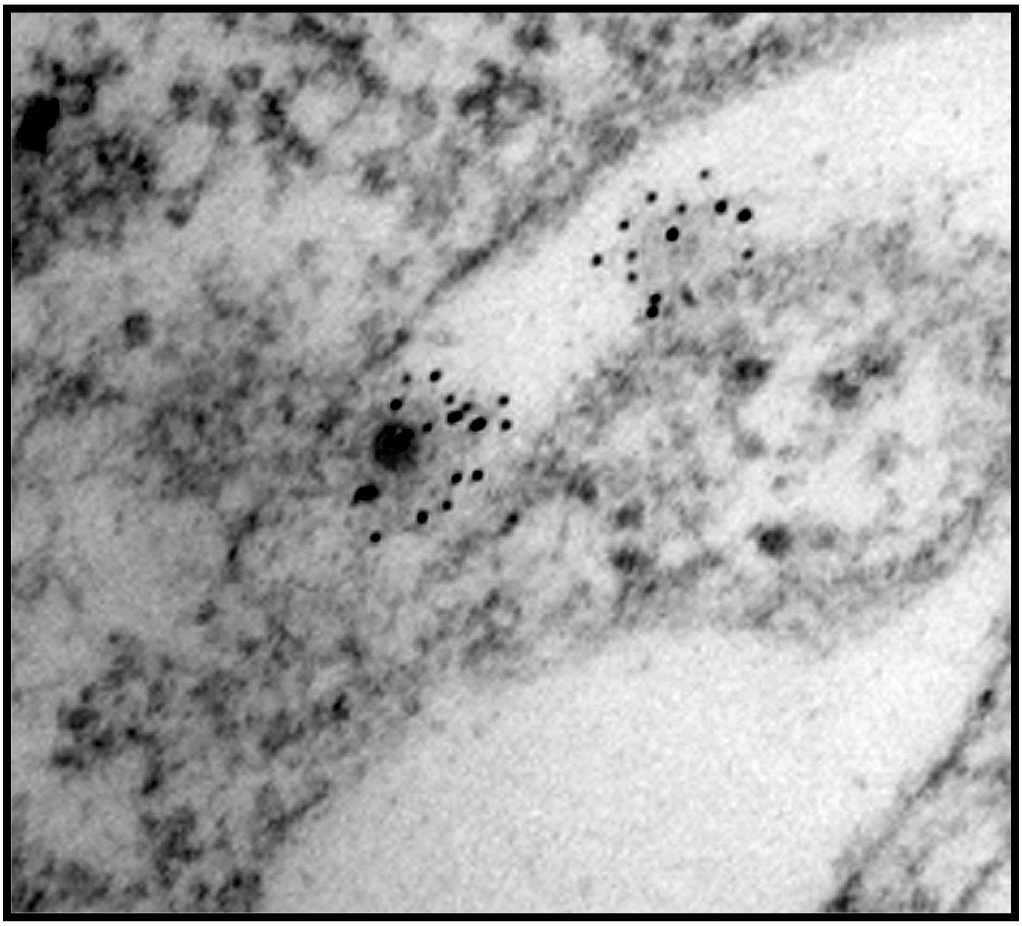

Figure 2.1: Sindbis virions lose their RNA content at the cell surface at neutral pH. Virus is labeled by antibody conjugated to gold beads (dark spots around viral particles).

stopped (Lippincott-Schwartz, Roberts, and Hirschberg, 2000). To further characterize the interaction of Sindbis virus with cells under conditions which block endocytosis, we examined the ability of the virus to establish infection at 5 ^{o}C and 15 ^{o}C. Our approach was to create an antibody escape experiment consisting of thefollowing steps: 1. A known quantity of virus was bound to identical monolayers of cells at 5 ^{o}C for 15 minutes (attachment). 2. The cells were washed to remove unbound virus and placed in media at either 5 ^{o}C, 15 ^{o}C or 22 ^{o}C for either 30 or 60 minutes (penetration). 3. The cells were then washed and incubated at 5 ^{o}C in media containing 0.4 mg/ml anti-SVHR whole virus IgG for 60 minutes (to inactivate virus particles which had not infected the cell or undergone a conformational change leading to infection) or in medium without antiserum. The antiserum used was polyclonal and the same as what was used in the electron microscopy studies of Paredes et. al. (2004, see also figure 2.1). In a virus inactivation experiment the antiserum inactivated 97% and 100% of virus infectivity in suspension in 15 and 30 minutes respectively at 5 ^{o}C in suspension. 4. The cells were then overlaid with agarose in media, incubated at 37 ^{o}C for 24 hrs. and stained with neutral red as in a standard plaque assay (Renz and Brown, 1976). In order to interpret the result of this experiment, it was necessary to demonstrate that the antiserum employed could inactivate virus particles after the virus had attached to the cell surface. This was done by following the protocol presented above but eliminating step 2, the penetration step. In this control experiment, we found that 13.9% of the virus attached to the monolayer formed plaques after step 3 (Fig. 2.2). The results of this

experiment are presented in figure 2.2. We found that significant numbers of virus particles could establish infection at low temperature. The overall levels of virus infection increased as temperature was increased from 5 ^{o}C to 15 ^{o}C and time was increased from 30 to 60 minutes. The majority of viral particles (97.7%) were capable of initiating the infection process at room temperature (22 ^{o}C) in 60 minutes, while this number falls to 78.4% if the incubation period is reduced to 30 minutes. A significant fraction of virions are also capable of initiating infection activity at 15 ^{o}C in 30 minutes (60.4%) and 60 minutes (72.4%). Even when the incubation is done at 5 ^{o}C we can detect viral infection in 28.3% and 35.7% of the virions, at 30 and 60 minutes respectively. These results indicate that events leading to the infection of cells can occur at temperatures which do not permit endocytosis and that this process occurred in a time and temperature dependent fashion yielding measurable kinetics of the infection reaction.

The results presented in figure 2.2 could alternatively be explained by the possibility that endocytosis is not blocked but rather slowed as temperature is lowered. While the effects of temperature on endocytosis have been extensively studied and no endocytosis is seen to occur at 15 ^{o}C, this parameter was measured in a standard assay of endocytosis which employs uptake of the vital dye neutral red (Long et al., 2005; Weeks et al., 1987). Neutral red is a large molecule that can be transported into living cells only by endocytosis. Equivalent monolayers of cells were treated with 0.00025% neutral red solution at the temperatures specified, for 30 minutes. The dyed cells were subsequently washed with cold buffer and the neutral

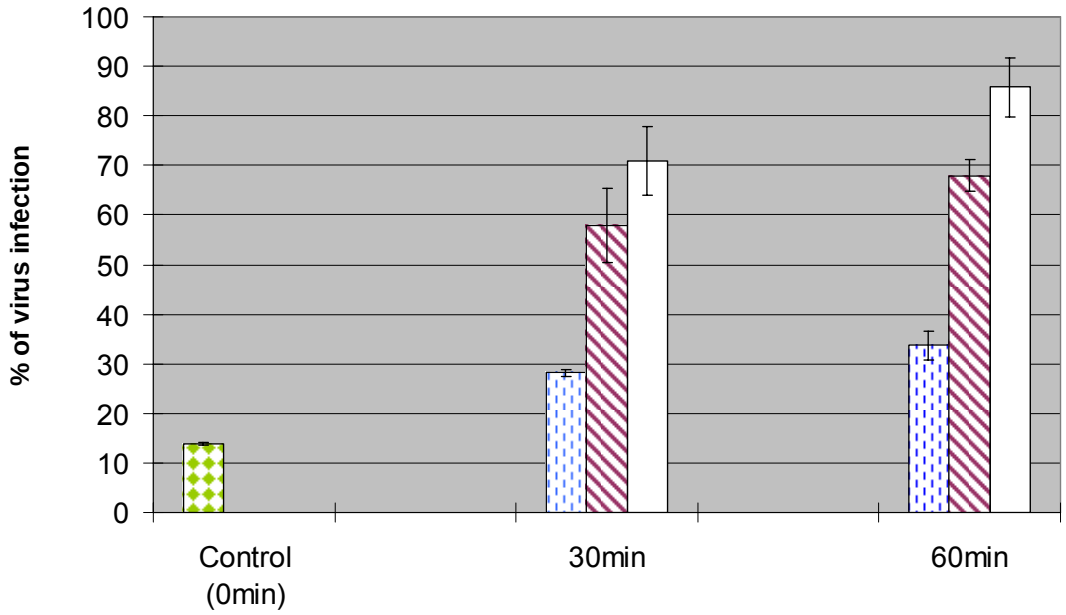

Figure 2.2: Formation of infectious centers by Sindbis virus at low temperature. Cells were infected with Sindbis, washed and exposed to antiserum as described in the text. The amount of virus which was able to infect cells under the conditions of time and temperature indicated was determined as the percentage of the total number of plaque forming units applied to the cell monolayers. The 0 time point at 5 ^{o}C is the control for the ability of the antiserum to inactivated virus after attachment to cells. Checkered: control. Squares: 5 ^{o}C. Chevron: 15 ^{o}C. White: 22 ^{o}C. Each entry is the average of three independent experiments. The error bars represent standard deviation of the data.

red was extracted from the cells with organic solvent (1:1 acetic acid/ethanol). The amount of cell associated neutral red was determined by measuring absorbance of the extract at 550nm. The results of these experiments are presented in figure 2.3. We found that at low temperatures (5°C, 10 °C and 15 °C), a low amount of neutral red was cell associated. This amount remained constant in all three of the lower temperatures tested. At temperatures of 22 °C and higher, a much greater amount of cell associated neutral red was recovered. A statistical analysis of the data produced gave a p-value of less than 0.0001 of the data from all six temperatures, which affirms a 99.99% confidence that the shift of neutral red uptake was not due to variance in the experiment. The same statistical procedure was applied to the subgroups of neutral red uptake data. Data from 5 °C, 10 °C and 15 °C experiments resulted in a p-value of 0.3664, while 22 °C, 28 °C and 37 °C gave a p-value of 0.2027. Thus, there is no significant difference among the three groups of data either below or above 15 °C. These data are in agreement with the observation that endocytosis is efficient at temperature of 22 °C and higher but raised the possibility that lower temperatures slowed but did not arrest the process of endocytosis. To examine this possibility we repeated the neutral red uptake experiment at 5 °C, 15 °C and 22 °C but included an experiment with cells at 22 °C which had been treated with 0.1M sodium azide for 30 min prior to the addition of neutral red. After 30 minutes, the amount of neutral red found associated with the azide treated cells at 22 °C was equivalent to that of the 5 °C and 15 °C live cells which were not treated by azide. These data suggest that the neutral red recovered from the low temperature cells is

due to background association and not to endocytosis. These data support the previous investigation demonstrating that endocytosis in mammalian cells does not take place at 15 ^{o}C or below.

The data presented above suggest that events leading to the infection of living cells by Sindbis virus can occur in the absence of endocytosis. We have proposed that these events also occur without the need for membrane fusion. To further examine this possibility we have determined if the phenomenon of Sindbis virus mediated cell-cell fusion can take place at low temperatures. We have previously shown that in contrast to fusion of virus with artificial liposomes, fusion of wild type virus with living cells does not occur at acidic pH but requires a return to neutral pH (Edwards and Brown, 1986; Paredes et al., 2004). We examined the ability of Sindbis virus to fuse BHK cells at 15 ^{o}C and 37 ^{o}C using standard procedures described previously (Edwards and Brown, 1986; Paredes et al., 2004). The result of this experiment is presented in figure 2.4. We found that at 15 ^{o}C, no evidence of cell fusion could be detected. At 37 ^{o}C, significant fusion of the cell monolayer was seen.

The use of low temperatures to block endocytosis and other events related to vesicular transport has been widely employed by cell biologists to study these processes (Lippincott-Schwartz, Roberts, and Hirschberg, 2000). We have used the benign mechanism of lowering the incubation temperature to establish conditions for studying the roles of vesicular transport/endocytosis in the penetration of cells by Alphaviruses. While we employed the measurement of a late event (virus production

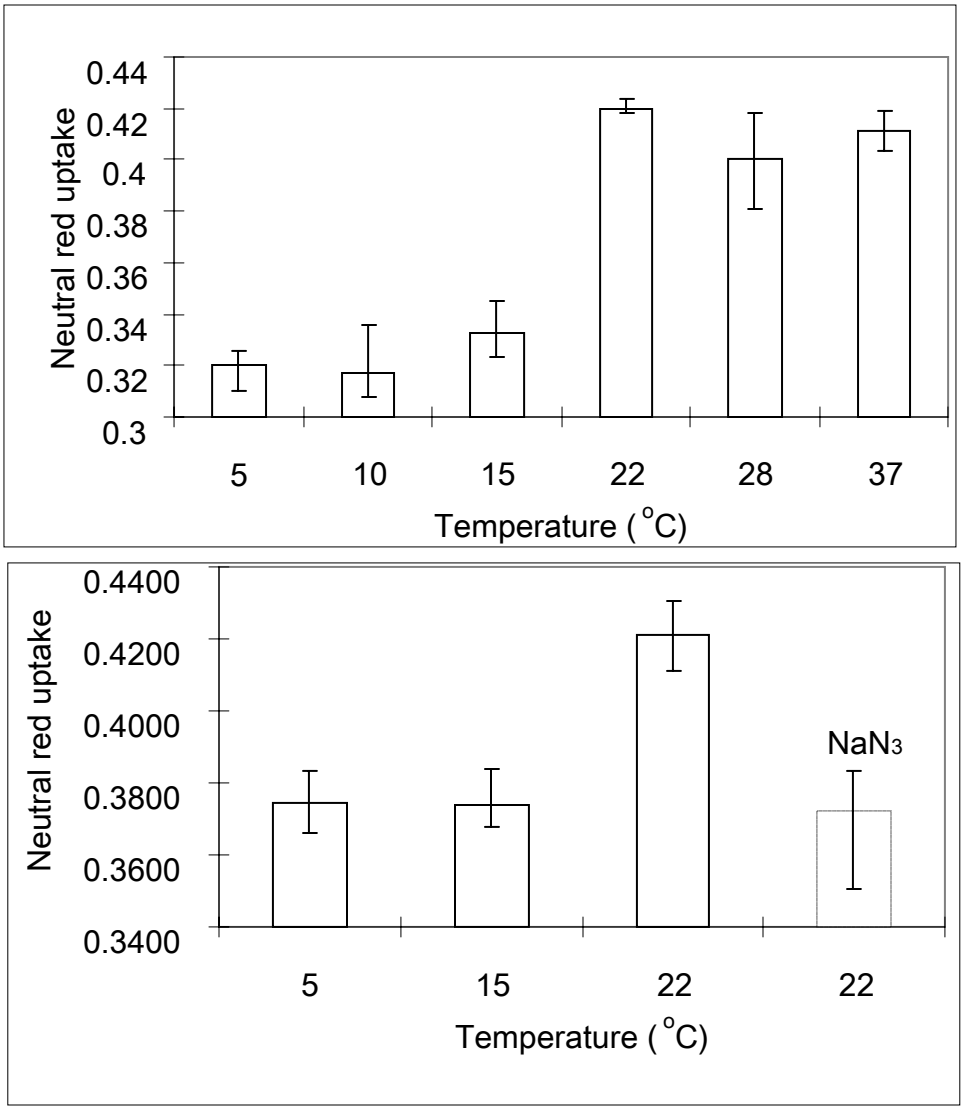

Figure 2.3: Uptake of neutral red by BHK cells at different temperatures. Cells were preincubated at the temperature and treated with neutral red in PBS-D for one hour, followed by a wash and extraction of the dye with organic solvent. Concentration of neutral red in the final solution is determined by measuring absorbance at 550nm. Error bars represent the range of data from three independent experiments. Noted in dashed column are data from cells pretreated by 0.1 M sodium azide for 30 minutes.

in a plaque assay) and other researchers also employed the assay of alternate virus replication events (RNA or protein synthesis as indicators that penetration had taken place). Our result differs from previous reports in that the data is positive indicating penetration must have taken place rather than a negative result (indicating that an event not related to penetration did not occur). In the case of a negative result, many known factors and unknown host cell mediated responses may have been involved.

The data presented above suggest that interaction of virus with living cells at low temperature allows for conformational changes in the virion which place the virus beyond inactivation by antivirus serum. The serum employed in this study was polyclonal and rapidly neutralized virus in solution. The antiserum was the same reagent used in the immuno gold-labeling experiments examining the process of Sindbis virus infection by electron microscopy (Paredes et al., 2004). In that EM study, we found that this antiserum could bind to virus which had lost its electron dense core and presumably had delivered its RNA into the host cell (see also figure 2.1). That observation suggested that the antiserum could bind to virus after RNA penetration and after protein conformational changes related to that process had taken place. We expect that the ability to bind virus in various states is retained in this study and that the escape from inactivation by antibody seen in figure 2.2 is likely not due to an inability of the antibody to bind a virion which has attached to cells and undergone structural rearrangements. The data presented in this paper add to a developing body of information suggesting that Alphaviruses can penetrate

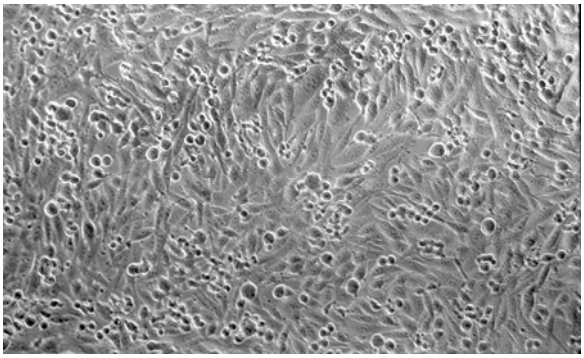

37 °C, pH5.3 pH5.3

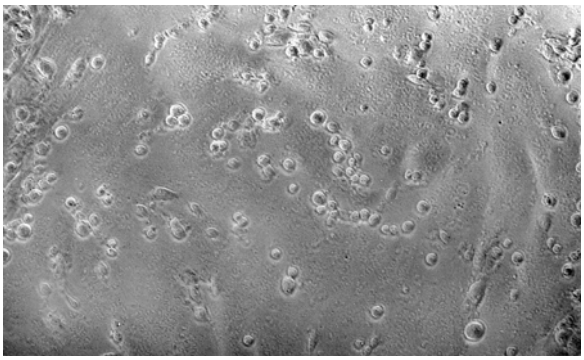

37 °C, pH5.3 pH7.4

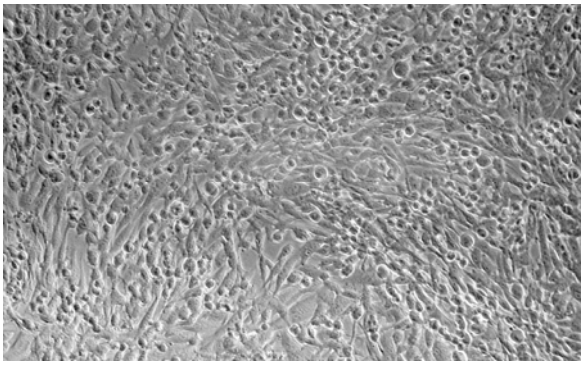

15 °C, pH5.3 pH5.3

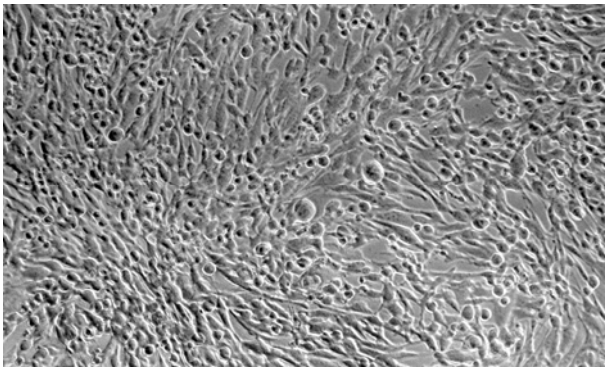

15 °C, pH5.3 pH7.4

Figure 2.4: Virus mediated cell-cell fusion at different temperatures induced by pH switches. Virus particles were added to cell monolayer at a Multiplicity of Infection (MOI) of 1000 viral particles per cell and rocked on ice for an hour for attachment. Infected cells were then incubated in low pH media (pH5.3) for 5 minutes, followed by return to neutral pH for another hour at that same temperature.

cells by a mechanism that does not require endocytosis, exposure to acidic pH or high concentrations of cholesterol in the target membrane (Koschinski et al., 2005; Paredes et al., 2004; Rietveld et al., 1999). The observation that events leading to infection can be initiated at low temperature, conditions which also prevent membrane fusion, support the notion that penetration occurs by production of a protein pore in the cell plasma membrane (Koschinski et al., 2005; Paredes et al., 2004). Evidence for the existence of such Sindbis virus induced pores produced in the plasma membranes of infected cells has existed for some time established by the observation that the newly infected cell becomes leaky and ion permeable (Ulug et al., 1984). This observation has been confirmed recently in experiments elaborating differences in pores formed as a result of penetration and pores formed as a result of membrane modification by virus proteins (Koschinski et al., 2005). Electron microscopy has also indicated the presence of a hollow connector developing between the virus and the cell surface during infection (Paredes et al., 2004). The early cytopathic effect in living cells exemplified by changes in ion permeability is in direct contrast to the fusion between virus and liposomes induced by low pH which is found to be non-leaky (Smit et al., 2002).

The difference in the structure of the envelope glycoproteins which make up the Type I and Type II “fusion” proteins suggest that while both classes of proteins are capable, under very specific conditions, of producing fusion of the virus membrane with a target membrane, they may function differently during the process of infection. Both types of proteins are capable of engaging cell membranes but

Type I fusion proteins which are capable of inducing a fusion event may differ from Type II fusion proteins. Type II fusion proteins may, in concert with the virus receptor, produce a protein pore in the host cell membrane. Infection of host cells by “Type II” proteins which are found in membrane containing viruses that must infect both vertebrates and invertebrates may require that they employ structural proteins in a very different ways to breach the barrier presented by these very different membranes. That the alternate, insect host, is poikilothermic and functions at ambient temperature may explain the ability of the Alphaviruses to infect cells at low temperatures.

CHAPTER 3

Introduction of the green fluorescent protein gene into the Sindbis virus genome as a reporter of successful infection

In the antibody escape experiment discussed in chapter 2, we carried out most of the treatments at low temperatures and added antibody at the last step to stop infection. After antibody treatment, virus particles should settle into two categories: those that have started the infection process before antibody addition and the others that have not. The virus particles that escaped antibody treatment should reproduce themselves in the infected cells and form plaques by spreading out and killing the peripheral cells. Those virions that did not get a chance to complete the initial steps of infection should be bound by antibody molecules and lose the ability of infection. By comparing the number of plaques formed in the sample treated with antibody to that of no-antibody treatment, we could calculate the percentage of infection that had occurred before addition of antibody. In that experiment however, we had to bring the cells to 37 ^{o}C after antibody treatment and overlay the cell monolayers with agarose in media so that we could count plaques. The assay part of the experiment was actually finished after antibody treatment. Raising the temperature to 37 ^{o}C was only for counting plaques and should not affect the assay result.

By contrast, at low temperatures such as 15 ^{o}C , neither cells nor viruses can grow. Although we can not evaluate successful infection rate of Sindbis virus by incubating cells at 15 ^{o}C in a plaque assay, we can use other technology into our system to observe the cells and virus infection at low temperatures. To test our hypothesis further with even more stringent conditions, we designed an experiment in which we could avoid any exposure of infected cells to temperature warmer than

15 ^{o}C. We introduced ZsGreen gene, a derivative of *Zoanthus sp.* green fluorescent protein gene, into the wild type Sindbis viral genome (Figure 3.1). Then we infected Baby Hamster Kidney (BHK) cells with this newly constructed virus. When we did both the infection and incubation at temperatures no higher than 15 ^{o}C, we detected with the help of laser microscopy the presence of green fluorescent protein.

Expression and maturation of green fluorescent protein at 15 ^{o}C

The green fluorescent protein (GFP) gene was bought from Clonetech. It came in the DNA form, vectored in a pUC19 plasmid backbone. In this plasmid, named pZsGreen, the GFP gene is under the control of the LacZ operon. The gene itself encodes a protein that is the derivative and brighter version of *Zoanthus sp.* green fluorescent protein. *Zoanthus sp.* is a species of corals that can grow on reefs and express green fluorescent protein at 20 ^{o}C in the sea. The protein needs a maturation step after expression to form tetramers before becoming fluorescent. The reported "maturation time" between transfection and seeing obvious green fluorescence provided by the vendor is 8-12 hours at 37 ^{o}C (Clontech, product information sheet).

To evaluate the expression and maturation process of GFP, we transformed the commercial vector that GFP gene resides into E.coli cells, grew the culture and measured bulk green fluorescence versus time. A 10-ml culture of bacterial cells containing pZsGreen was grown overnight in LB media containing 1% glucose. Glucose is the inhibitor of LacZ operon. In the presence of glucose, GFP gene is not

expressed. Then the culture was split into two equal volumes. One of them was kept in 1% glucose as the control. IPTG was added to the other one to induce gene expression controlled by the LacZ operon. We did this experiment at both 15 ^{o}C and 37 ^{o}C. In 5 hours at 37 ^{o}C, massive maturation of GFP began (Fig. 3.1). After 10 hours, the production and degradation of GFP tetramers reached equilibrium. The amount of GFP plateaus from this time on, until the last time point recorded.

While at 15 ^{o}C, the maturation process takes much longer time (Fig. 3.2). No GFP was detected until 20 hours post-induction and the concentration of GFP fades quickly. The highest concentration of GFP reached in bacteria at 15 ^{o}C is only one tenth that seen at 37 ^{o}C (Fig. 3.1, Fig. 3.2). Part of this difference is due to the growth of bacteria at 37 ^{o}C and absence of bacterial self-replication at 15 ^{o}C. A general approximation we can get from the graphs is that metabolism slows at 15 ^{o}C to require triple the time at 15 ^{o}C compared to 37 ^{o}C. Although metabolism is much slower at 15 ^{o}C, we have confirmed that green fluorescent protein can be synthesized and maturate at 15 ^{o}C (Fig. 3.2).

Introduction of the green fluorescent protein gene into Sindbis viral genome

The GFP gene is about 700bp in size, one fifteenth of the wild type Sindbis virus genome. Genetic engineering was used with double stranded plasmid DNA to manipulate the GFP gene. There are XbaI restriction sites on both sides of the GFP gene in its commercial vector, pZsGreen, and are the only two XbaI restriction sites in the plasmid. The gene was cut out of its original commercial vector using these

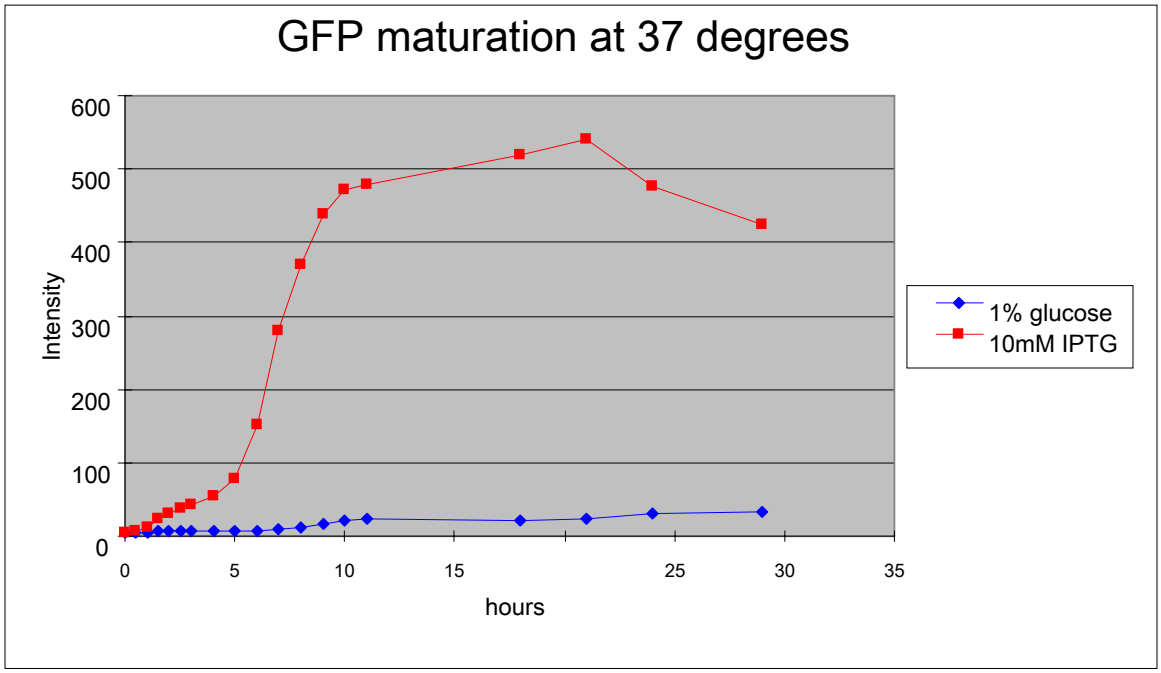

Figure 3.1: Expression of GFP gene in bacterial cells at 37 ^{o}C. The same source of bacterial cells containing GFP gene in the plasmid were split into two at the 0 time point. In the control, lacZ operon was inhibited by 1% glucose. Expression of GFP was induced by the addition of IPTG. Samples were kept shaking in a 37^{o}C incubator. Expression of GFP was quantified by measuring absorbance at 505nm with excitation at 493nm in a fluorometer.

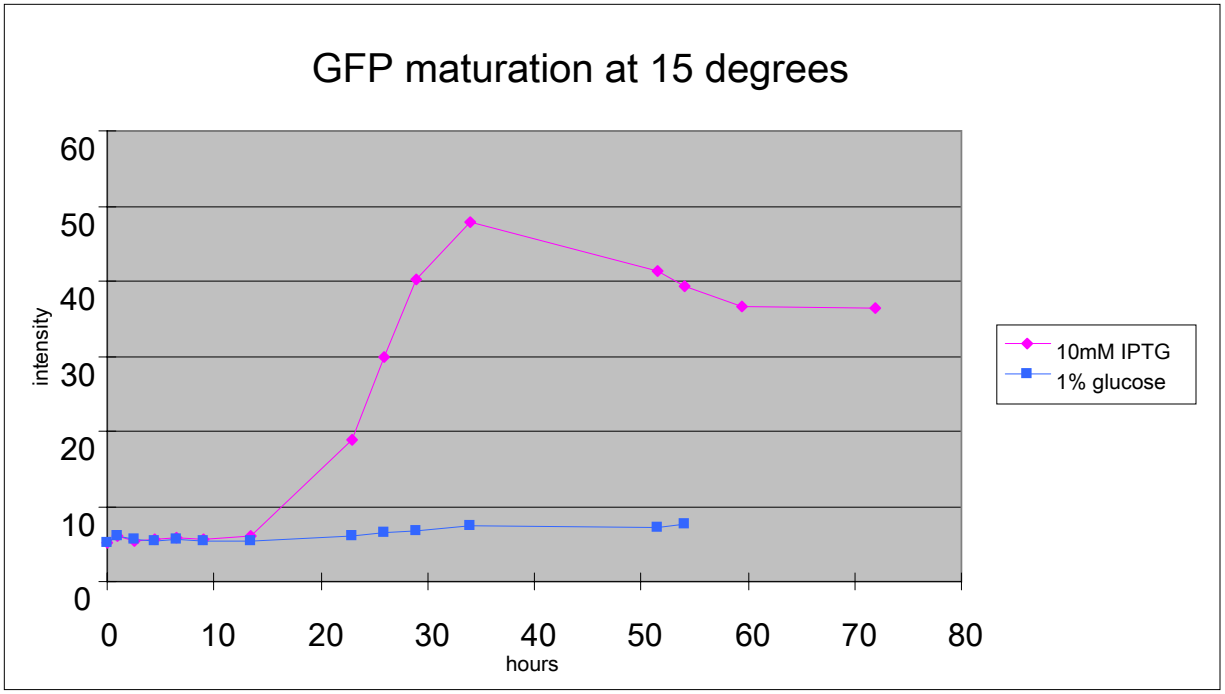

Figure 3.2: Expression of GFP gene in bacteria cells at 15 ^{o}C. Same source of bacteria cells containing the GFP gene in the plasmid were split into two aliquots after the log phase was reached. In the control, lacZ operon was inhibited by 1% glucose. Expression of GFP was induced by addition of IPTG. Samples were kept shaking in 15 ^{o}C incubator. Expression of GFP was quantified by measuring absorbance at 505nm with excitation at 493nm in a fluorometer.

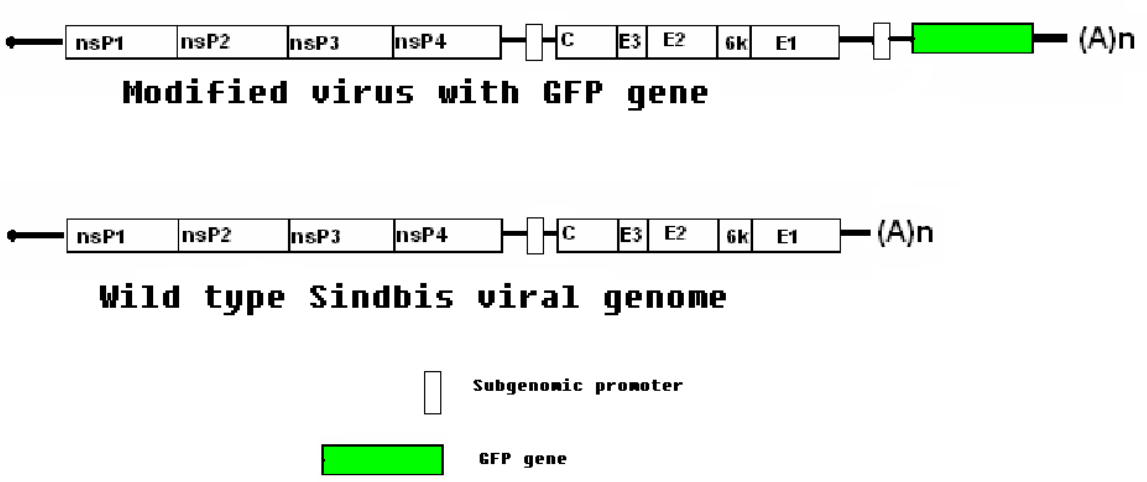

Figure 3.3: Genome organization of wild type Sindbis virus and modified virus with the GFP gene. The wild type viral genome has 11703 nucleotides. The GFP gene is about 700 nucleotides long.

two XbaI sites. pTE3'2J is a plasmid DNA that contains all the genomic information of Sindbis virus. At the 5' end of the viral genome between the structural protein genes and poly-adenylated tail, there is a repeated subgenomic promoter. pTE3'2J also has a unique XbaI cutting site, which is located between this extra subgenomic promoter and poly-adenylated tail. GFP gene was introduced into pTE3'2J plasmid by a ligation reaction. The product DNA was then transformed into E.coli cells. The colonies containing product DNA with GFP gene at the correct orientation were screened out by PCR.

Production of "green virus" from plasmid DNA clone

As the first step in making virus from plasmid DNA, DNA was linearized using the unique XhoI restriction site. Full length viral genomic RNA was produced by in vitro transcription using SP6 RNA polymerase, followed by transfection into BHK cells.

The "green virus" from the transfection has an infectious virus titer of 1.36×10^7 Plaque Forming Unit/ml (PFU/ml), which is similar to the wild type control value of 2.33×10^7 PFU/ml. Cells transfected with this newly constructed virus show green fluorescence under laser microscopy (data not shown). This confirms successful expression of the GFP gene as a part of the Sindbis virus infection. This construct was shown to express high infectivity when incorporated into the virus particle and also expressed all genes in transfected cells.

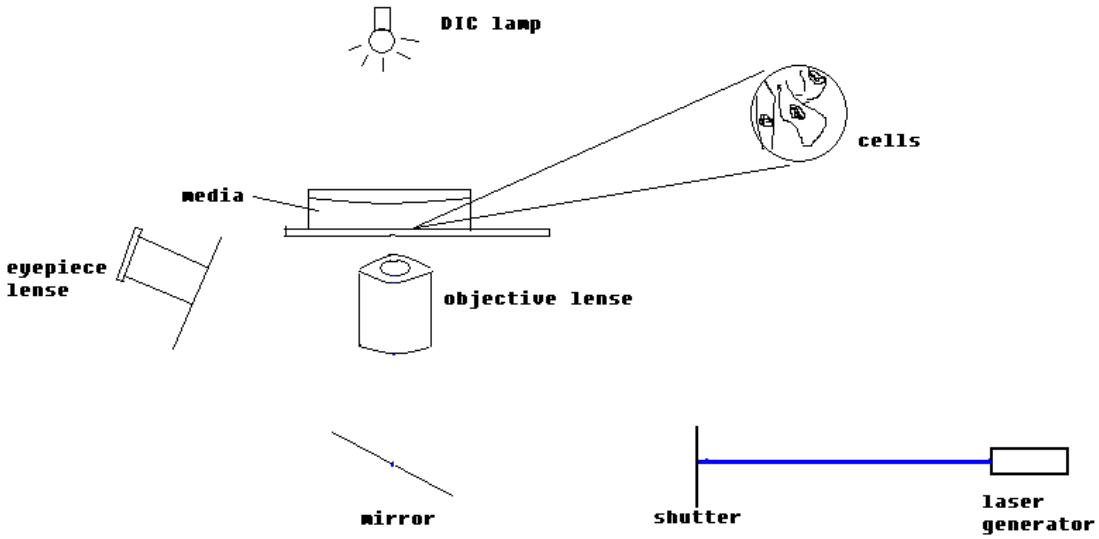

Figure 3.4: The normal inverted microscope mode. The differential interference contrast (DIC) lamp must be turned on for this mode. Sample images can be observed by eye or using a camera connected to a computer.

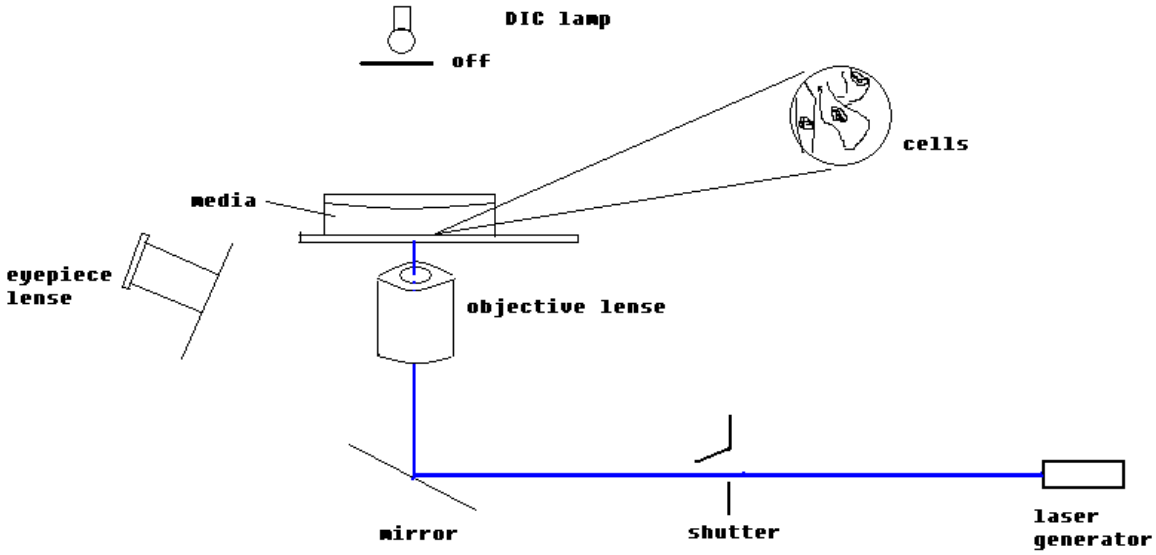

Figure 3.5: The laser fluorescent mode of the microscope. The laser mode is controlled by a shutter. Laser activated fluorescence from the sample can be observed by eye or alternatively by a camera connected to a computer.

Real-time laser microscopy observational system

To look at virus infection at the single-cell level, we exploited a real-time laser microscopy observational system. A schematic representation of how the system works and how it switches between the two modes is shown in Figures 3.4 and 3.5.

The microscope can be used as an inverted microscope to look at cells by Differential Interference Contrast (DIC) mode (Fig. 3.4). In this mode, the laser beam is blocked before entering the system. The DIC lamp is the light source. Image of cells can be seen through the eyepiece lens. There is also a camera connected as the alternative observation pathway (not shown in the figure). The camera can receive the signal and pass it onto a computer. Software on the computer can show the images and collect data as images or movies.

By controlling the on and off of the shutter, we can shoot the laser beam perpendicularly through the center of the lens. With the DIC lamp off, the system switches to the laser-fluorescence mode. In this mode, the laser is the light source that activates fluorescence energy in the sample. The fluorescent signal is then transmitted through the lens into the observational path. Before the signal reaches the eyepiece lens or camera, a filter in the light path makes sure only light at the correct wave length can penetrate. This setup is to get rid of the image of unnecessary background fluorescence from the cells. In our experiment, a blue laser is used to activate fluorescence from mature GFP. Data in image or movie form were collected by computer software.

Infection of BHK cells by "green virus" at 37 ^{o}C

With the virus and observational system ready, we infected cells with the modified "green virus" and incubated the samples at 37 ^{o}C. BHK cells infected by this modified virus can express green fluorescent protein at 37 ^{o}C as observed by laser microscopy (Fig. 3.6). After the cells were infected by wild type virus, we could see a normal cell monolayer in DIC mode (Fig. 3.6 A). When we looked at this same area under the laser mode, we could only see the blue background (Fig. 3.6 B). The cells infected by "green virus" do not look different under DIC mode (Fig. 3.6 C). However, these cells have potent green fluorescence under a blue laser (Fig. 3.6 D). The camera in this system can only measure the strength of signal at each pixel, but not the colors. The colors in the image generated by computer software represent different strengths of the signal. The dark red area has the strongest green fluorescence. The yellow area has less green fluorescence than the dark red area, but more than the bright blue area. The blue area is background.

The titer data and laser microscope observation results confirmed that the virus we constructed with an extra gene can infect cells with almost wild type virus efficiency and that infected BHK cells are capable of expressing the introduced green fluorescent gene at 37 ^{o}C.

Infection of BHK cells by "green virus" at 15 ^{o}C

The preliminary data show that GFP can be expressed and form fluorescent tetramers at 15 ^{o}C, although the rate is much slower (Fig. 3.2). At 37 ^{o}C, virus can

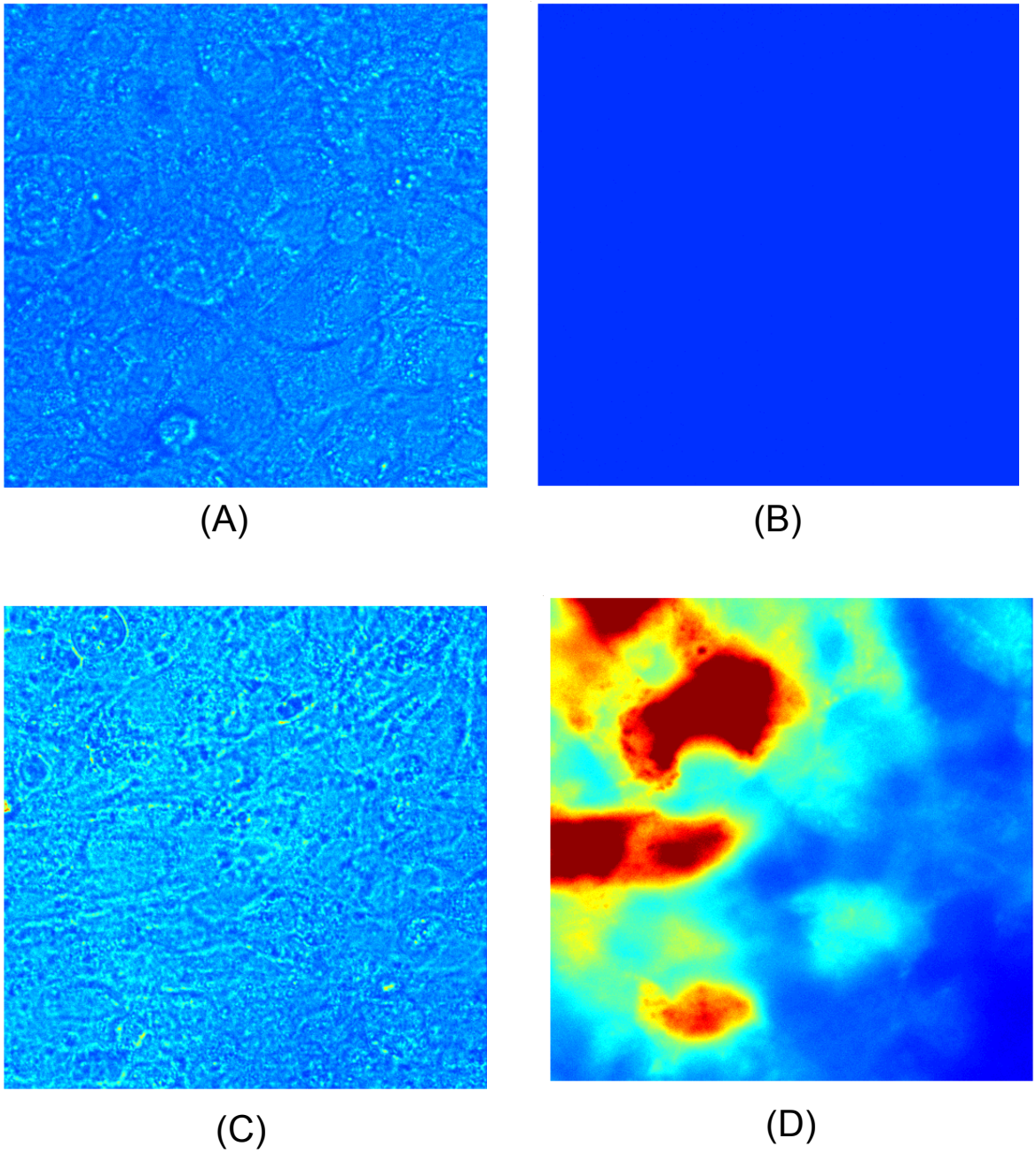

Figure 3.6: Cells infected by “green virus” express green fluorescent protein at 37 ^{o}C within 24 hours post-infection. (A) DIC image of cells infected by wild type virus. (B) Same area as in A under the laser. (C) DIC image of cells infected by modified virus containing the GFP gene. (D) Same area as in C under laser. Blue laser (473nm) is used to activate GFP. Signal from the sample went through a 505nm filter so that only green fluorescence is detected.

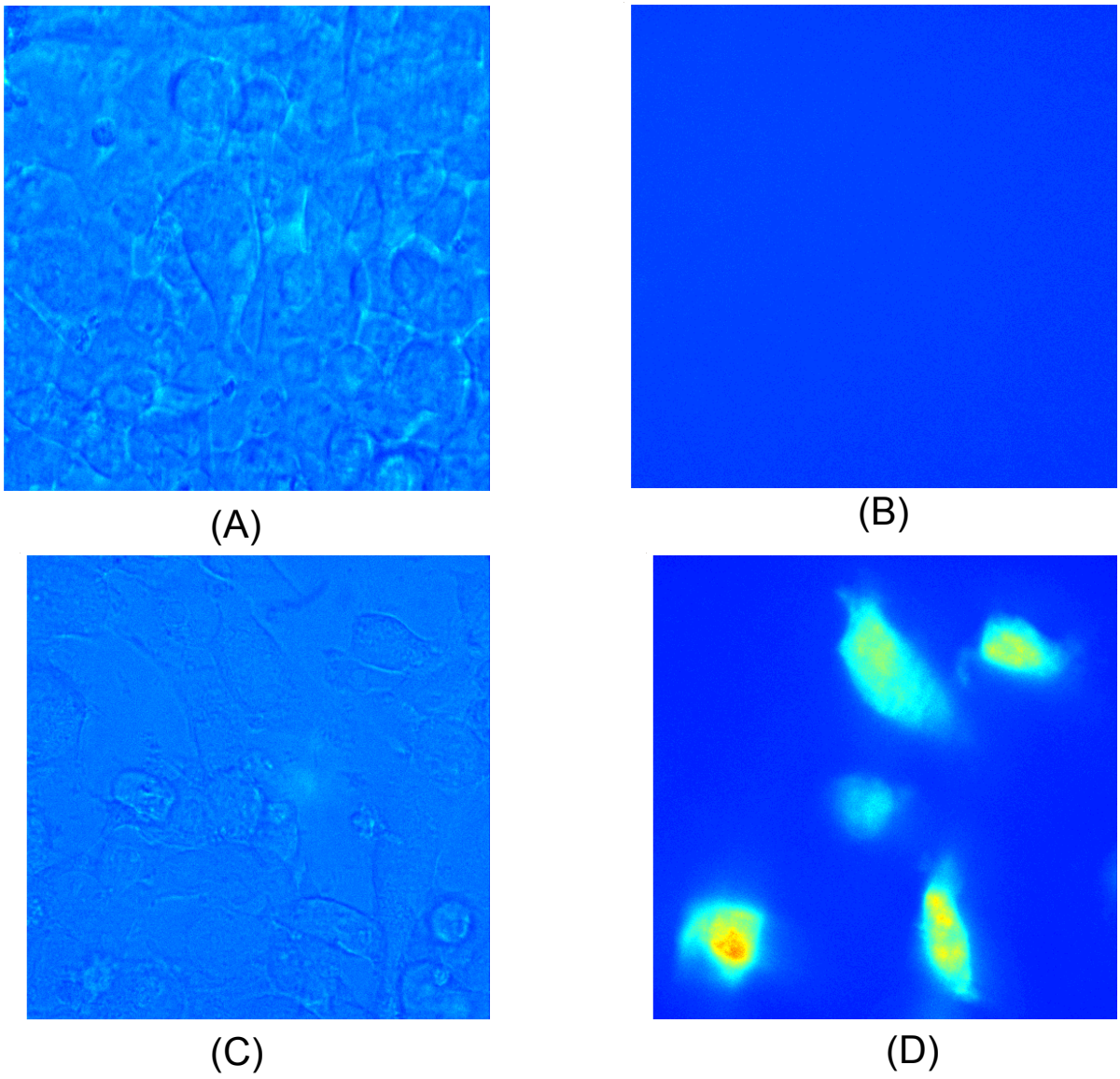

Figure 3.7: Cells infected by “green virus” express green fluorescent protein at 15 ^{o}C at 72 hours post-infection. (A) DIC image of cells infected by wild type virus. (B) Same spot as in A under laser. (C) DIC image of cells infected by modified virus with GFP gene. (D) Same spot as in C under laser. Blue laser (473nm) is used to activate GFP. Signal from the sample went through a 505nm filter so that only green fluorescence is recorded.

infect cells, replicate and spread into the media to infect more cells. At 15 ^{o}C, however, all vesicular transport is inhibited. Virus infection of one cell may not lead to infection of neighboring cells. Additionally, the virus life cycle at lower temperatures is longer than normal. All these aspects of the low temperature experiment make it harder to detect GFP-positive cells than at 37 ^{o}C. Virus harvested from a transfection is concentrated enough to do an infection and allow us to see the majority of cells turn green within 18 hours at 37 ^{o}C. A small portion of infected cells may reproduce and circulate virus so that most of the cells become green in 18 hours at this temperature. When the same concentration of virus was added to cells and incubated at 15 ^{o}C, only a few green cells from a field of 100,000 cells were detected.

Multiplicity of Infection (MOI) is an index to control the average infectious virus particles added per cell. This number is very important when we do low-temperature infection, as the successful infection rate is very low. Several protocols for purifying and concentrating virus to maintain the required Multiplicity of Infection (MOI) were tested. We transfected green virus RNA into BHK cells and used the virus produced to do a large scale infection. Then we used iodixanol as the gradient medium (Ford T., 1994) to concentrate virus from the large scale infection. Iodixanol is iso-osmotic to both virus and cells. We used iodixanol in purification and infection does not harm the virus or cells. These properties were helpful in the low-temperature experiment to optimized infection. We infected BHK cells on ice and

incubated infected cells at 15 ^{o}C in fresh media. After 72 hours, we detected cells that expressed GFP (Fig. 3.6).

Discussion

The result from this experiment shows that Sindbis virus can release its viral RNA into the host cell at 15 ^{o}C and the viral genome can be expressed in an infection at this temperature. This confirmed our previous finding that at 15 ^{o}C Sindbis virus can infect BHK cells. This protocol is a better experiment because the cells and virus were never exposed to warm temperatures after infection. This experiment completely rules out the possibility of infection initiation by endocytosis. Paredes and colleagues sought to answer this question with the help of electron microscopy (Paredes et al., 2004). In that study virus was added to cells at neutral pH followed by the addition of polyclonal antibody against Sindbis. The antibody molecules were conjugated to gold beads so that the antibody molecules could be visualized as dark spots. In the images produced by their experiment, viruses surrounded by antibodies can be located on the cell surface. After attaching to the host cell, viruses may lose or still retain their RNA content. Intervening between some of the viral particles and the host cell, tubular structures were seen. There is a pore-like structure formed at the interface from what appears to be the 5 fold axis. A closer look at the pore-like structure reveals that it visibly extends from the cell to the virion surface. The tubular structure closely contacts both the virus body and infected cell, connecting the two together.

In addition to pore structures found in both empty and RNA containing particles, Paredes and colleagues observed the flow of density presumably from the inside of virus into the pore portion. The observed particle is a Sindbis virion as it is surrounded by specific antibody molecules. The resolution seen in an EM thin-section can define the cell boundaries, which confirmed that the virions were at the cell surface. The image obtained may be of an intermediate stage in the process of viral RNA injection into the cell.

Alphaviruses and flaviviruses are close relatives. Both virus groups belong to the arboviruses. There are over 700 known members of this group including Yellow Fever Virus, Dengue Fever Virus, West Nile Virus and many encephalitic viruses. There are about 100 million cases of diseases annually caused by arboviruses. Understanding the precise entry mechanism is critical for the prevention of viral infection and disease.

Our data suggest an entry mechanism that does not require endocytosis or fusion. We propose a direct penetration process at the cell plasma membrane at neutral pH by Sindbis virus. This scenario starts when virus binds to a cell receptor. The binding may promote a local or overall conformational change in the outer surface protein shell of virus. A pore structure is then formed in the presence of cell receptor, forming a channel between the virus and host cell. The conformational changes required for pore formation may be related to a localized acidic environment, provided by the cell receptor. The highly packed viral genome is then

released into the cell cytosol and disassembled as this would be energetically favorable.

Chapter 4

Impact of deletions in the Sindbis virus E1 transmembrane domain on virus function

Introduction

Sindbis virus is the prototype of *Togaviridae* family, *Alphavirus* genus. It is propagated in nature by blood sucking insect vectors such as mosquitoes, ticks and midges. The virus can be transmitted from natural reservoirs such as rodents and birds to domestic animals and humans. Insects that take blood meals from animals can transmit the virus to other mammalian individuals. But Sindbis virus cannot grow to high concentration during a viremia in humans. Thus enough virus can not be provided in a blood meal from humans for insects to transmit the virus to other targets. This is due to the potent immune response possessed by humans against Sindbis virus infection and does not cause any human disease.

The mature Sindbis virion has two protein shells with a host derived membrane bilayer sandwiched in between. The inner nucleocapsid shell, containing viral genomic RNA, is built from 240 copies of capsid protein. The outer shell is composed of two glycoproteins, E1 and E2. E1 and E2 form heterodimers which trimerize. There are 80 trimers in each Sindbis virion. E1 and E2 have transmembrane domains which traverse the membrane bilayer. E2 contains a cytoplasmic “tail” so that it can make direct contact with the nucleocapsid to maintain the rigid structure of a virus. The outer shell has 240 copies of E1-E2 heterodimer. Both shells have icosahedral symmetry with a triangulation number of 4. The outer shell icosahedral symmetry is a reflection of the inner shell due to the well defined interaction between capsid protein and the E2 endodomain.

The structural proteins including capsid, E1 and E2 are synthesized as one polyprotein from the subgenomic mRNA on cytoplasmic ribosomes, NH-C-E3-E2-6K-E1-COOH. After capsid protein is removed by autoproteolysis, the RNA-ribosome is associated with the endoplasmic reticulum where the rest of the polyprotein is made and incorporated into the membrane with multiple transmembrane domains. En route to the plasma membrane, the polyprotein is processed by signal peptidase and furin proteinase activity to form a trimeric complex. Nucleocapsids are assembled in the cytoplasm and package a single strand of genomic RNA. During maturation, nucleocapsid associates with the endodomain of E1-E2 complexes which are found in the plasma membrane. This interaction directs the budding process of virus particles.

E1 and E2 proteins have 436 and 423 amino acids, respectively. The predicted transmembrane domains are 24 to 28 amino acids in length. The transmembrane domains are important not only for correct protein expression and dimerization, but also for the transportation from endoplasmic reticulum to the plasma membrane during which time appropriate cleavage and post-translational decorations are completed. To determine the residues involved in the endodomain binding reaction, chimeric alphavirus with structural proteins from Sindbis and Ross River viruses were constructed. The chimera virus is composed of Ross River E1, Sindbis E2 and Sindbis capsid protein produced low titers of infectious virus. Passage of the chimeric virus until wild type titers were achieved were selected for revertants that restored virus titer (Strauss, Lenches, and Strauss, 2002). The

structural proteins in the revertants were sequenced to elucidate amino acid substitutions. This research revealed several positions in the transmembrane domains of E1 and E2 that are critical for viral infectivity. Amino acid substitutions at these positions restored viral infectivity at least two orders of magnitude. This observation suggests that the hydrophobic anchors may establish critical interaction between E1 and E2 for virus assembly and function.

To characterize the role of E2 in tansmembrane domain interactions, sequential deletions in the E2 transmembrane domain were first made (Hernandez et al., 2003; Whitehurst et al., 2006). Most of these deletions do not impair assembly, but infectivity. It was also concluded from this research that the length of E2 transmembrane domain is essential for infectivity rather than the specific amino acid sequence.

Incremental deletions in the E2 transmembrane domain (26 amino acids long) show that virus infectivity is not positively correlated to its length (Hernandez et al., 2003). Instead, with more amino acids deleted from the region, the titer follows a cyclic pattern of increasing virus titer in both mammalian and mosquito cells. One single amino acid deletion dropped the titer by four orders of magnitude. However, the titer was restored gradually when more amino acids were deleted until there were 18 amino acids remaining in the transmembrane domain. The mutant with only 18 amino acids in the domain had the same titer as wild type virus which has 26 amino acids in the E2 transmembrane domain. Virus titer dropped again when more than 8 amino acids were deleted from the region. There was a partial restoration of

virus titer when 12 or 16 amino acids were deleted. Surprisingly, when big deletions such as 14 and 18 amino acids were made from E2 transmembrane domain, there was still virus production, although the titers were low.

To investigate the mechanism by which one amino acid deletion dropped virus titer by four orders of magnitude, single deletions in different regions of the E2 transmembrane domain were produced. The position of single deletion on different angles of the helix does not have different effects on virus titer. However, deletions closer to the carboxyl terminus are more detrimental than the ones near the amino terminus.

E1 transmembrane domain deletion mutants (Fig. 4.1 & Fig. 4.2)

To complete the characterization of the E1-E2 transmembrane domain interaction, a series of deletions in E1 transmembrane domain were constructed (Fig. 4.1). The infectivity of these mutants determined by plaque assay is shown in Figure 4.2.

Deleting one methionine in the E2 transmembrane domain dropped virus titer by four orders of magnitude (Hernandez et al., 2003). Single deletions near the carboxyl terminus of E2 transmembrane domain have a dramatic effect on virus infectivity (Whitehurst et al., 2006). Therefore we deleted one methionine at position 433 from the carboxyl region of E1 transmembrane domain. Surprisingly, there was no titer drop for this mutant. Next, both methionines near the carboxyl terminus

E1Δ433: WSWLFALFGGASSLLIIGLMIFACSMML

E1Δ432-433: WSWLFALFGGASSLLIIGLMIFACSMML

E1Δ422: WSWLFALFGGASSLLIIGLMIFACSMML

E1Δ422-423: WSWLFALFGGASSLLIIGLMIFACSMML

E1Δ413-414: WSWLFALFGGASSLLIIGLMIFACSMML

E1Δ420-433: WSWLFALFGGASSLLIIGLMIFACSMML

E1Δ411-428: WSWLFALFGGASSLLIIGLMIFACSMML

E1Δ416-433: WSWLFALFGGASSLLIIGLMIFACSMML

Wild type (Y420): WSWLFALFGGASSLLIIGLMIFACSMML

Figure 4.1: The E1 transmembrane domain amino acid sequence of wild type Sindbis virus and deletion mutants. Underlined and colored are the deleted amino acids from the region.

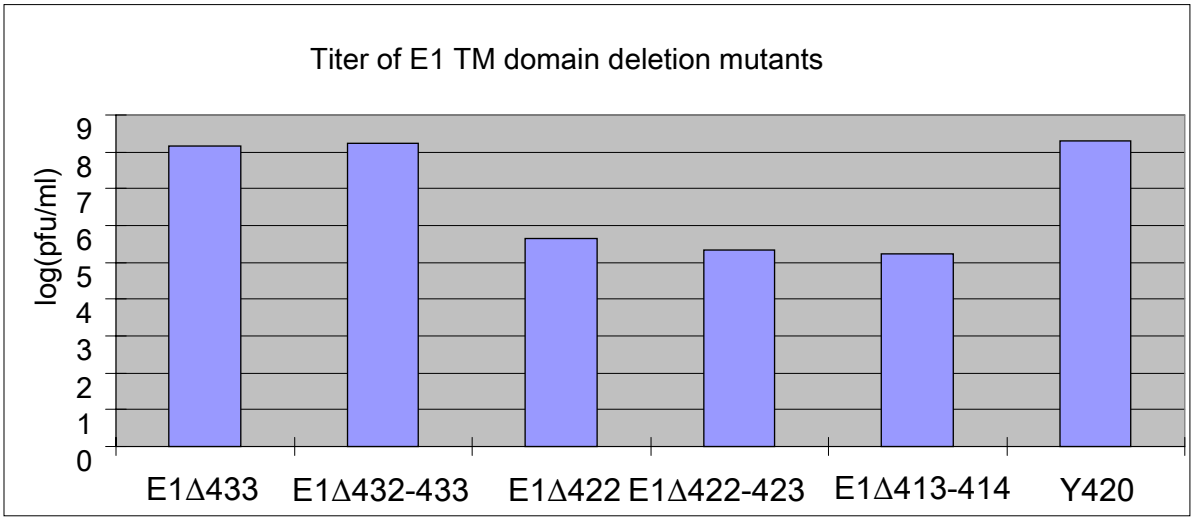

Figure 4.2: Virus infectivity determined by plaque assay. Viral RNA was transfected into BHK cells. Virus was harvested by collecting the media and titrated immediately.

were deleted. The mutant with both methionines deleted produced the same titer as wild type.

There are two isoleucines in E1 transmembrane domain. They are the 422nd and 423rd moieties in the E1 protein amino acid sequence (Strauss, Lenches, and Strauss, 2002). The position occupied by these isoleucines had been shown to be important for E1-E2 interaction. The isoleucine at position 422 was deleted. The virus titer dropped by three orders of magnitude. Deleting the second isoleucine did not drop the virus titer further, compared to the single isoleucine deletion.

Deleting amino acids at the distal and proximal regions of the E2 transmembrane domain resulted in differential virus infectivity (Whitehurst et al., 2006). Thus two amino acids were deleted from the E1 amino terminus (E1Δ413-414). A titer drop of three orders of magnitude is observed.

Large deletions of 14 and 18 amino acids from the E1 TMD were also constructed. Deletions were made near both the amino (E1Δ411-428) and carboxyl termini (E1Δ420-433, Δ416-433). Unlike the E2 transmembrane domain deletion mutants, mutants with large deletions in E1 did not produce any infectious virus (data not shown). There are several possible explanations for this discrepancy between E1 and E2 large deletion mutants. First, Sindbis virus structural proteins are originally synthesized as a polyprotein, in which E1 and E2 occupy different positions. E1 and E2 are both integrated into the endoplasmic reticulum membrane during the process of polyprotein synthesis, followed by enzymatic cleavage that separates them. E1 is at the carboxyl terminal end of the polyprotein, while E2 is

centrally located. When large deletions in the E2 transmembrane are made, the topology of the protein may allow the transmembrane domain to remain membrane associated since both ends of the polyprotein are initially membrane anchored. There may be an adjustment of local membrane thickness that compensates for this abnormal protein. When the same number of amino acids is deleted from E1, the membrane association may not be of sufficient stability to hold the protein in the membrane. This would lead to failure of E1 integration or retention into the membrane bilayer. Secondly, E1 and E2 endodomains are of different sizes. The endodomain of E2 has 33 amino acids, while E1 has only 2 amino acids in the cytosol. When the same number of amino acids is deleted from both transmembrane domains, E2 is known to have more flexibility (data not shown) in retracting part of its endodomain into the transmembrane domain to compensate for deleterious effects. The E2 endodomain also helps in anchoring the protein in the membrane prior to reorientation.

The E1 deletion mutants can be categorized into two groups: the short deletion mutants that produced infectious particles and large deletion mutants that did not produce any infectious virus. The two groups were characterized.

Characterization of short deletion mutants

One important index used to characterize these mutants is particle to Plaque Forming Unit (PFU) ratio. Each infected cell can produce ~10^6 virus particles. However, not every virus assembled is infectious. For every virus strain, certain

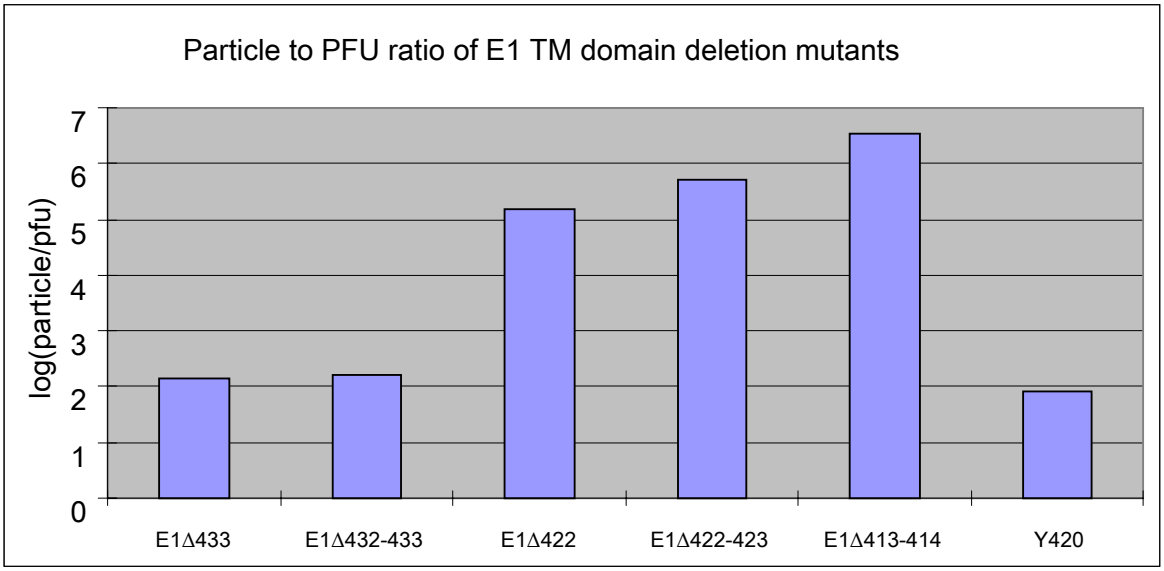

Figure 4.3: Particle to PFU (plaque forming unit) ratio of the mutants with short deletions in E1.

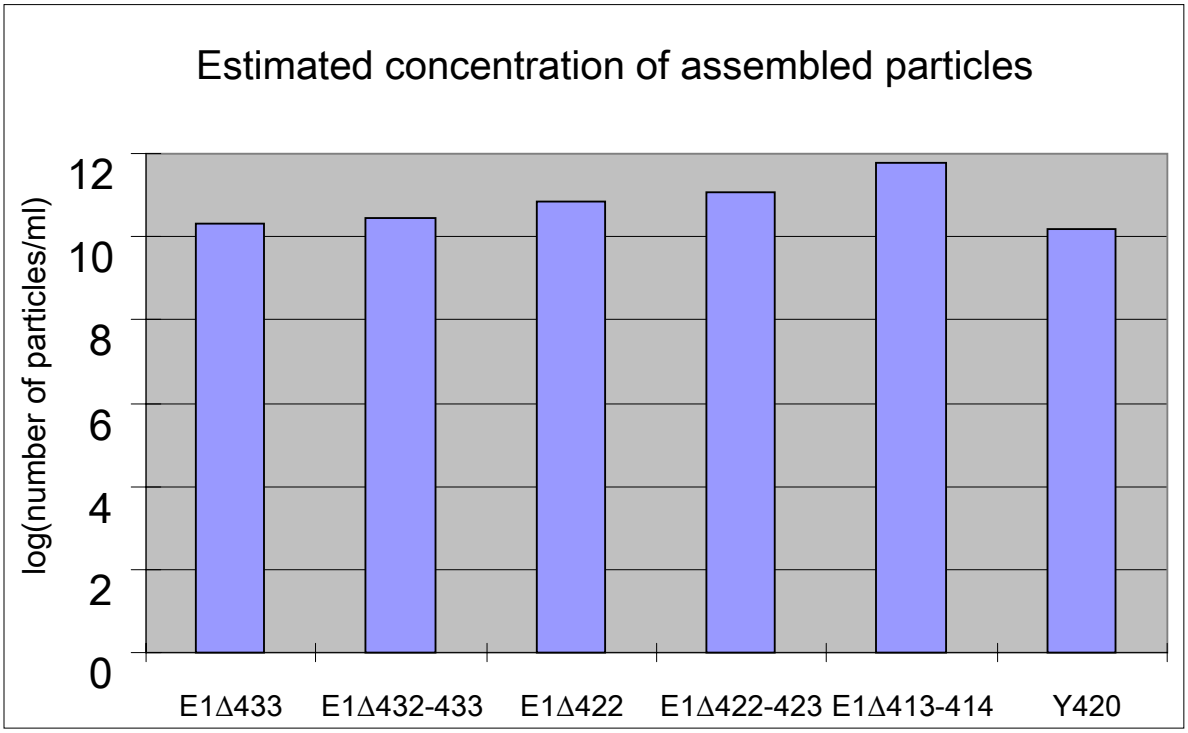

Figure 4.4: Estimated concentration of assembled particles. The concentration of particles is estimated by multiplying virus titer and particle to PFU ratio.

numbers of particles are required to form one plaque on average. As the large deletion mutants did not produce any infectious particles at all, only the particle to PFU ratios of short deletion mutants could be determined (Figure 4.3). Y420 is the wild type control in this experiment. This wild type strain has a particle to PFU ratio of about one hundred. The methionine deletion mutants (E1Δ433, E1Δ432-433) have approximately the same particle to PFU ratio as the wild type control. However, the isoleucine deletions (E1Δ422, Δ422-423) have an elevated particle to PFU ratio. The mutant with deletion near amino terminus (Δ413-414) has an even higher particle to PFU ratio.

The titer and the particle to PFU ratio data are used to estimate virus assembly and infectvity. The transfection products are amplified during a subsequent infection. To determine the particle to PFU ratio, virus harvested from the infection is purified on step and continuous tartrate gradients. The unit of plaque assay titer data is PFU per ml. The unit of particle to PFU is the actual number of particles which are required to produce one plaque (PFU). These two numbers can be multiplied to calculate particle concentration in the original transfection stock. The estimated concentrations of assembled virus particles for the short deletion mutants are shown in Figure 4.4. Although different infectious virus titers were obtained from these mutants, the concentration of particles assembled for each strain is similar. This suggests that the E1 short deletion mutants do not affect the assembly process of the virus, as evidenced by the concentration of viral particles produced. Instead,

the ratio of infectious virus in the population determines the overall infectivity of a strain.

Characterization of mutants with large deletions in E1 transmembrane domain

The E1 large deletion mutants did not produce any plaques in the plaque assay. This was not seen in the E2 transmembrane deletion mutants (Hernandez et al., 2003). Further investigation into which step of the virus life cycle is affected by these deletions was necessary.

The Sindbis virus life cycle starts with attachment, penetration and uncoating. The non-structural proteins near the 5'-end of the viral genome are expressed first. After enough non-structural protein is synthesized, genome replication and structural protein synthesis occurs in the cytosol and endoplasmic reticulum respectively. Assembly and budding are the final steps of the virus life cycle. Since the deletions were made in the structural proteins, the initial replication steps of infection are unlikely to be impaired. Analysis of the phenotypes of these mutants began with assays of viral structural protein synthesis, nucleocapsid assembly and budding.

To assay viral protein synthesis, Baby Hamster Kidney (BHK) cells were transfected with mutant viral RNA. Then synthesized protein was labeled metabolically by ^{35}[S] radioactive isotopes. Viral protein was isolated from the cellular proteins using poly-clonal antibody conjugated to protein A beads. Viral protein was then solubilized in buffer and run on an SDS-PAGE gel (Fig. 4.5). Our results show that protein expression is not impaired by the E1 transmembrane

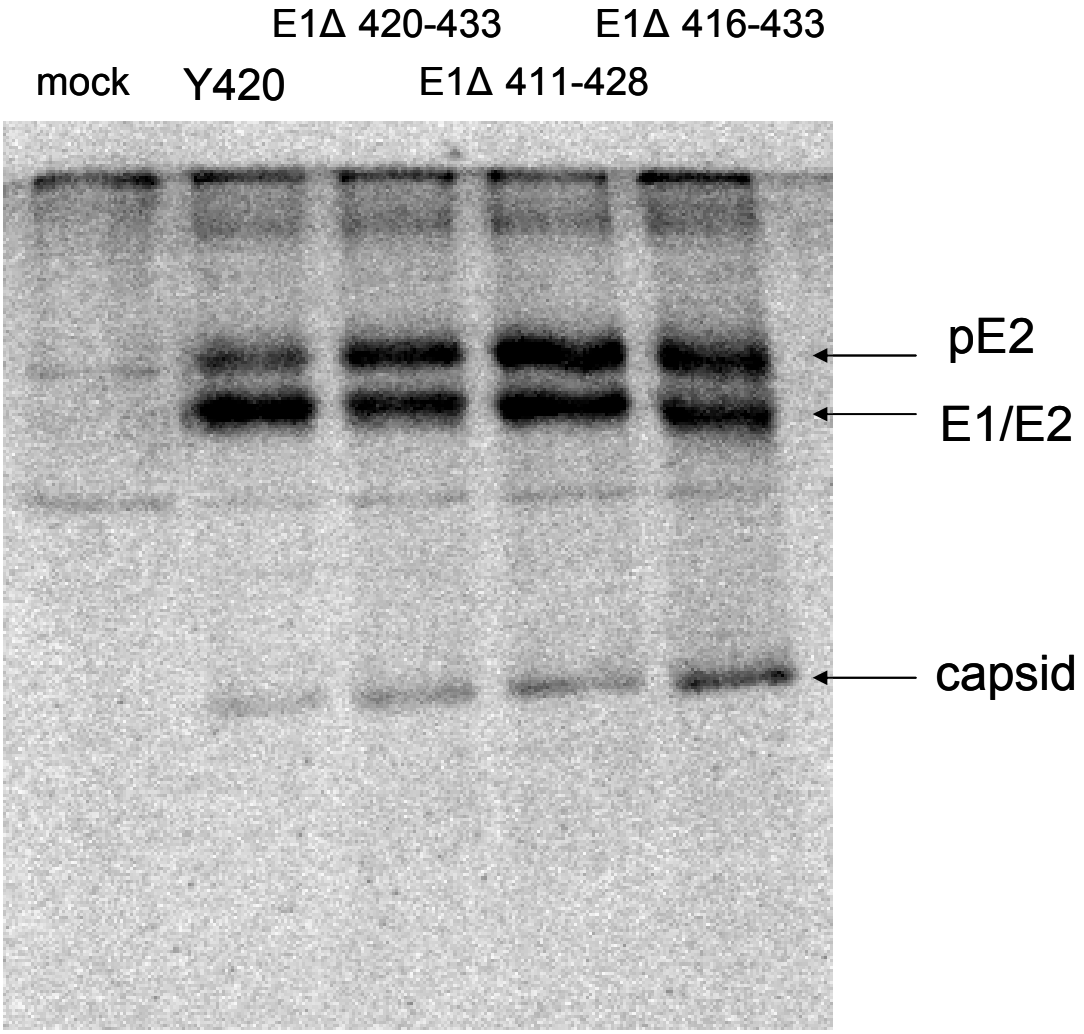

Figure 4.5: Viral protein synthesis in mutants with large deletions in the E1 transmembrane domain.

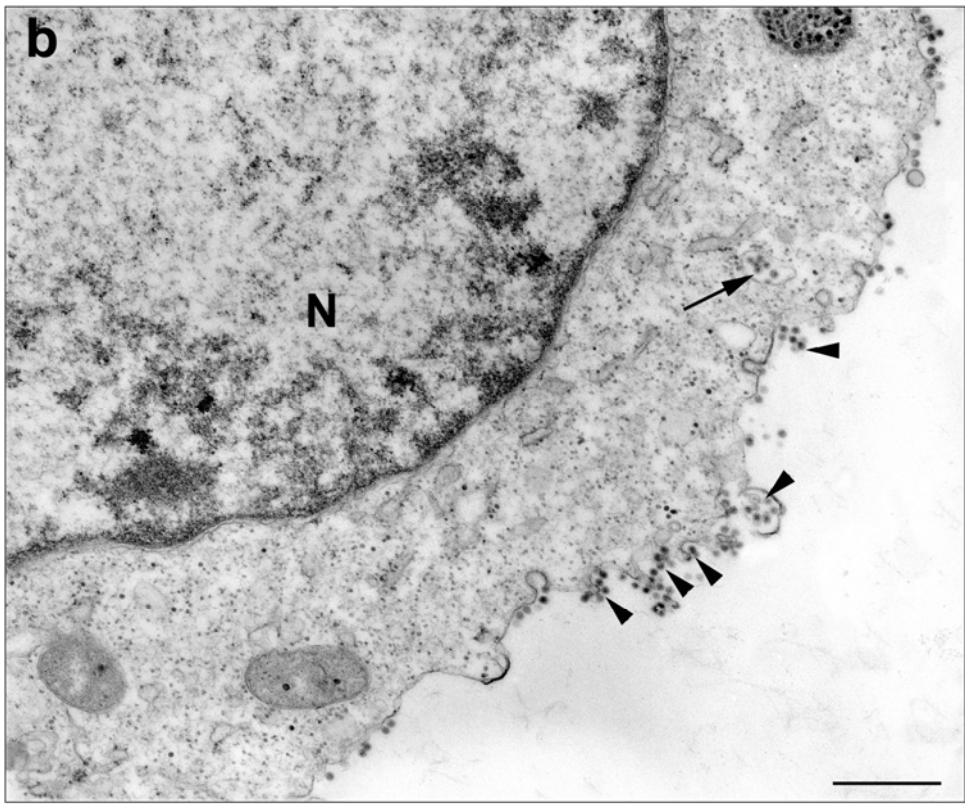

Figure 4.6: Wild type virus assembly and budding in BHK cells. N denotes the nucleus. The arrow points to conjugates of nucleocapsid in the cytoplasm. The arrow heads point to sites at the plasma membrane where budding occurs. The bar in the lower right corner of the picture is 630nm long.

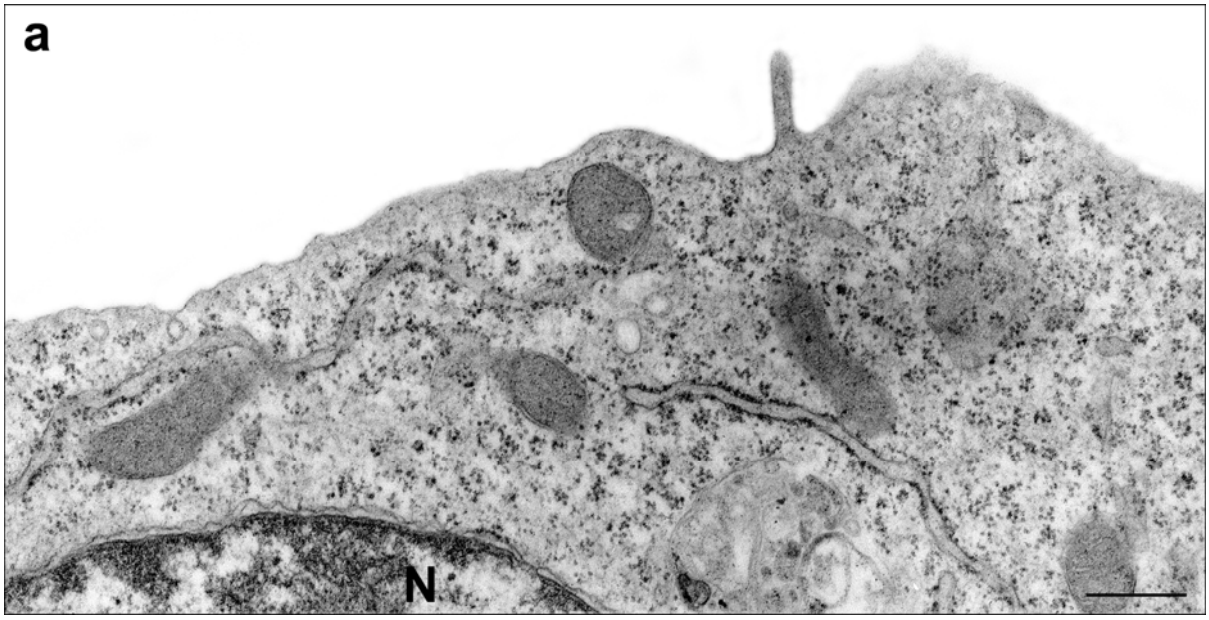

Figure 4.7: BHK cells transfected with non-viral RNA. N stands for nucleus. There is no nucleocapsid assembly or budding. The dark dots are ribosomes in the cytosol. The black bar at the lower right corner represents a length of 630nm.

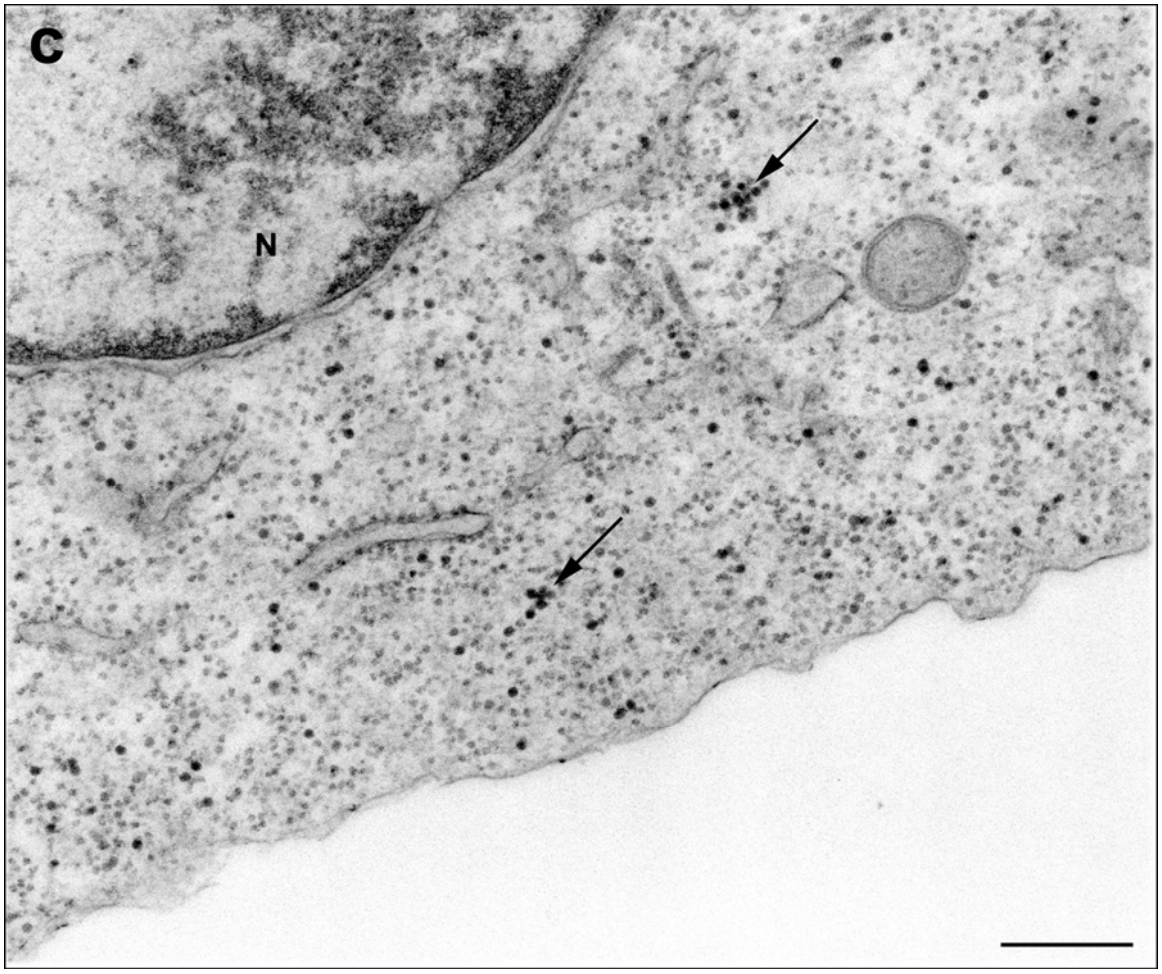

Figure 4.8: BHK cells transfected with E1Δ420-433 RNA. N stands for nucleus. The arrows point to assembled nucleocapsids. The bar at lower right corner represents a length of 630nm.

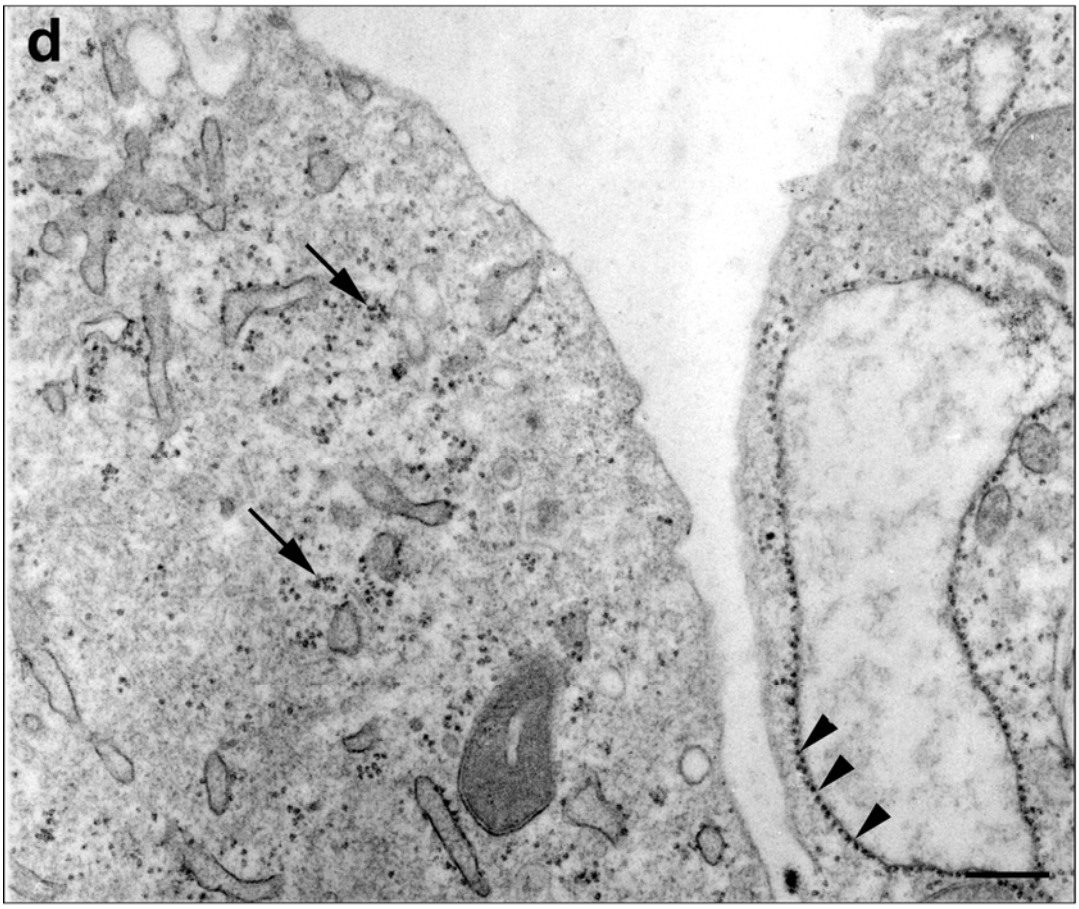

Figure 4.9: BHK cells transfected with E1Δ411-428 RNA. N stands for nucleus. The arrows point to assembled nucleocapsids. The bar in the lower right corner represents a length of 630nm.

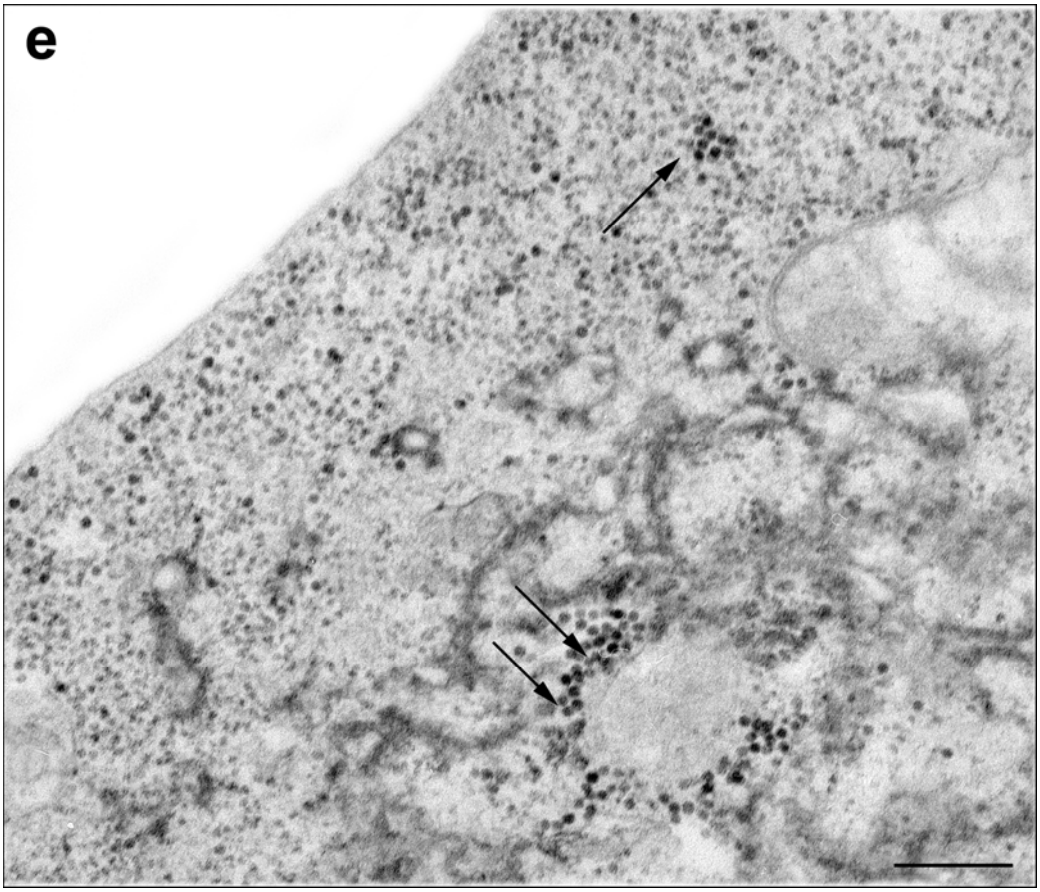

Figure 4.10: BHK cells transfected with E1Δ416-433 RNA. N stands for nucleus. The arrows point to assembled nucleocapsids. The bar in the lower right corner represents a length of 630nm.

deletions. The structural proteins are being synthesized in the expected ratios. In wild type virus, the band of pE2 is not as strong as E1/E2 band. While in the mutants, the darkness of the two bands is about the same. This suggests that the maturation process from pE2 to E2 is not as active in these mutants. It is unlikely that the short deletion mutants would cause a malfunction in protein expression, as there was significant infectious virus production from each of them.

Because the synthesis of structural proteins is not impaired, the next thing to assess is nucleocapsid assembly and virus budding. To look at nucleocapsid assembly, viral RNA was transfected into BHK cells, followed by fixation of the samples and thin sectioning. The ultrastructure of the infected cells was then observed under a transmission electron microscope. In the cells transfected with wild type RNA, there were assembled nucleocapsids in the cytosol and many sites of virus budding at the plasma membrane surface (Fig. 4.6). Cells transfected with non-viral RNA did not show any assembled virus particles or signs of budding (Fig. 4.7). Large deletion mutants were also transfected into BHK cells and evaluated. In all these mutants, nucleocapsid assembly was successful, but no virus budding was observed (Fig. 4.8, 4.9 & 4.10). The conclusion is that the large deletions are lethal to infectious virus production, because the virus budding process cannot be completed. Our data suggest that E1 protein with a much shorter transmembrane domain can still be synthesized. Our data also suggest that E1 proteins with large deletions may not be stable in the membrane, which leads to the failure of virus budding at the plasma membrane.

Conclusion

The above results can be interpreted and summarized in the following manner. The methionines near the carboxyl terminus in E1 are not as essential as their counterparts in the E2 TMD. Shortening the E1 TMD by 2 amino acids may have no effect on virus assembly or infectivity. The positions occupied by the isoleucines are important, as deleting even one of them dropped the virus titer by three orders of magnitude. In the E1 TMD, deletion near the amino terminus seems more detrimental than the ones near the carboxyl terminus. Short deletions in the E1 TMD do not impair the assembly process. Instead, they affect the function of assembled virus particles. Large deletions in the E1 TMD are lethal for virus function. However, the large deletions do not affect viral protein synthesis or nucleocapsid assembly. The impact of the large deletions in the E1 TMD may be on the stability of E1 in the membrane and final budding process in virus life cycle.

After combining the E1 and E2 data, we found an interesting phenomenon involving two identical adjacent pairs of amino acids that reside in the two proteins. The mutant TM25 has one methionine deleted from its E2 transmembrane domain. TM24 has both adjacent methionines deleted from the same region (Hernandez et al., 2003). E1Δ422 and E1Δ422-423 have one and two isoleucines deleted from the E1 transmembrane domain respectively. The titers of these four mutants are all similar (Hernandez et al., 2003). The particle to PFU ratios of these four mutants also close (Fig. 4.3). Additionally, these deletions are located in very close locations when viewed in the context of the transmembrane domain amino acid sequence (Fig.

4.11). These are also the most detrimental short deletions we have obtained in making E1 and E2 transmembrane domain mutants.

E1 and E2 TMD interactions

We constructed a mutant with both pairs of amino acids deleted. The amino acid sequence of the transmembrane domains in this mutant, named combined double deletion, is shown in figure 4.11. When we transfected this mutant with short deletions in both TMDs into BHK cells, there was no detectable virus production (data not shown). This suggests that the two pairs of amino acids are very important for the interaction between E1 and E2 TMDs. Such a dramatic drop in titer also increases the possibility that they facilitate critical interactions within different microdomains. We also looked at the ultrastructure of cells transfected with this mutant virus. We observed the assembly of nucleocapsids but no budding at the plasma membrane (data not shown).

Discussion

Deletions in the E2 TMD resulted in mutants that produced different titers in mammalian and mosquito cells in vitro. We will check if the E1 transmembrane large deletion mutants can produce virus in mosquito cells.

E1 TM domain

wild type: WSWLFALFGGASSLLIIGLMIFACSMML

E1Δ 422: WSWLFALFGGASSLL**I**IGLMIFACSMML

E1Δ 422-423:WSWLFALFGGASSLL**II**GLMIFACSMML

E2 TM domain

wild type: VYTILAVASATVAMMIGVTVAVLCAC

TM25: VYTILAVASATVAM**M**IGVTVAVLCAC

TM24: VYTILAVASATVA**MM**IGVTVAVLCAC

"Combined double deletion mutant"

E1 TM domain: WSWLFALFGGASSLL**II**GLMIFACSMML

E2 TM domain: VYTILAVASATVA**MM**IGVTVAVLCAC

Figure 4.11: Amino acid sequences of four E1 and E2 transmembrane domain deletion mutants. Underscored and colored letters represent amino acids deleted from the region.

CHAPTER 5

Methods

Cells and anti-Sindbis virus antibody

Baby Hamster Kidney (BHK-21) cells were propagated in minimal essential medium containing Earl's salts (Invitrogen, Carlsbad, CA) supplemented with 10% fetal bovine serum (FBS) (Invitrogen, Carlsbad, CA), 5% tryptose phosphate broth, and 2 mM glutamine as per standard protocol. Antibody against Sindbis viral proteins was produced in rabbits (Lampire, Pipersville, PA), and was the same as what was used in previously published electron microscopy studies (Paredes et al. 2004 and Figure 2.1). IgG was purified from serum using a HiTrap protein A column (Amersham, Uppsala, Sweden) (Paredes et al., 2004).

Virus growth and purification

Wild type Sindbis virus was grown in BHK-21 cells as described previously (Renz and Brown, 1976). Virus was twice purified by density gradient centrifugation on continuous potassium tartrate gradients. Purified virus was titrated on BHK 21 cells and infectivity (particle to PFU ratio) was determined as described previously (Hernandez et al., 2003). The infectivity of the virus employed in these studies was 3 virus particles per infectious unit.

Electron Microscopy

BHK cell monolayers were fixed with paraformaldehyde followed by fixing with 3% glutaraldehyde in 0.1 M cacodylic acid buffer, pH 7.4 (Ladd Research Industries, Williston, VT) at 4 ^{o}C. The cells were washed three times with 0.1 M cacodylic acid

and stained by 2% osmium tetroxide in cacodylic buffer for 1 hour. Cells were then washed as before and embedded in 2% agarose. The agarose containing the cell sample was then prestained with 1% uranyl acetate (Polaron Instruments Inc, Hatfield, PA) overnight at 4 ^{o}C. The samples were washed and carried through ethanol dehydration. Infiltration was done using SPURR compound (LADD Research Industries). Blocks were then trimmed on an LKB NOVA Ultrotome (Leica Microsystems, Inc. Deerfield, IL). Ultrathin sections were stained with 5% uranyl acetate in distilled water for 60 minutes and in Reynolds lead citrate, pH 12 (Mallinkrodt Baker Inc. Paris, KY) for 4 minutes. The samples were examined at 80 kV in a JEOL JEM 100S transmission electron microscope.

Low temperature infection initiation assay

Equivalent monolayers of BHK cells were grown in 25 cm^2 cell culture flasks at 37 ^{o}C. Virus was attached to cell monolayers at 5 ^{o}C for 15 minutes while rocking, followed by incubation at 5 ^{o}C, 15 ^{o}C or 22 ^{o}C for 30 or 60 minutes. After removal of the inoculum, purified IgG was added to the virus-cell mixture at 5 ^{o}C for 60 minutes to inactivate virions that had not yet undergone infection. Cells were then immobilized with agarose in media and kept at 37 ^{o}C, 5% CO_2 for two days before plaques were counted.

Antibody neutralization assay

To determine the efficiency of antibody employed in the experiments described in Figures 2.1 and 2.2 in virus inactivation, an antibody neutralization assay (plaque reduction neutralization titer) was carried out. Wild type virus was treated with the same concentration of antibody (0.04 mg/ml) as used in low temperature infection initiation assay for 60 minutes at 5 ^{o}C. Virus infectivity as measured by pfu/ml, was then determined in a standard plaque assay. Percentage of virus neutralized was computed by the reduction in titer of antibody treated virus versus the non-antibody treated control.

Neutral red uptake assay and spectral analysis

A neutral red uptake assay was employed to measure the ability of cells to take up macromolecules at different temperatures (Long et al., 2005; Weeks et al., 1987). To avoid crystal formation, neutral red solution was incubated in a 37 ^{o}C water bath overnight and filtered just before use. Cells were treated with 0.00025% neutral red in PBS-D and 3% serum for 30 minutes followed by a wash of cell monolayer using ice-by cold PBS-D. Cell associated neutral red was extracted using a 1:1 ratio of ethanol and acetic acid. Absorbance of the extract was measured at 550nm using a Beckman DU 7500 spectrophotometer. All assays were done in triplicate. P-values were generated by the ANOVA procedure in SAS 8.0.

PCR screening for transformed colonies with GFP gene in the correct orientation

After GFP gene was introduced into pTE3'2J plasmid DNA by XbaI restriction sites, colonies with successful transformation were screened by the selective marker on pTE3'2J that is resistant to carbenicillin. The plasmid DNA was extracted by Wizard® Plus Miniprep DNA Purification System from Promega, WI, USA. As the sticky ends are the same on both sides of the GFP gene, it may ligate to the vector in two orientations. To screen for DNA with GFP in the correct orientation, the samples of the correct size were further screened by PCR. In the PCR reaction, one primer binds to the negative strand near the 3' end of GFP gene and the other primer binds to the positive strand on the vector upstream of the GFP gene. If the GFP gene was in the right orientation, a PCR product of 900bp in size was obtained. Otherwise, no PCR product is seen. Out of the 11 colonies we picked from the plates, 6 had the GFP gene in the correct orientation. The final product DNA was also checked by sequencing.

Transfection of Sindbis virus into BHK cells by electroporation

BHK cells were washed by PBS-D and trypsinized, followed by multiple washes of RNase-free PBS-D as in Hernandez *et al*. Then the cells were resuspended in PBS-D and the concentration of cells was determined by counting on a hemocytometer. The volume was adjusted by PBS-D to reach a final concentration of $1\text{-}2\times10^7$ cells/ml. For each RNA sample, 400 µL of these cells were used. The electroporation was done in a 2 mm cuvette using a Bio-rad gene pulser™. The settings on that machine were 1.5 KV, 25 µF capacitance and ∞

resistance. The cells were then transferred into 10 ml of the appropriate media and settled down in a 25 cm^2 flask. Virus was collected 24 hours post-transfection.

Virus sample preparation, infection and observation of 15 ^oC infection

Viral RNA was transfected into BHK cells by electroporation. Virus produced was harvested at 24 hours post-transfection when cytopathic effect (CPE) was observed. Harvested virus (10ml) was added to ten 75 cm^2 flasks of BHK cells and rocked for an hour. The inoculum was discarded and 7 mls of media was added to each flask. Then virus was collected after CPE was seen and concentrated on a step gradient using iodixanol in PBS-D (pH7.4). The two concentrations used for the step gradient were 12% and 30% of iodixanol. The The virus sample was then titrated immediately and added to cells pre-incubated at 15 ^oC. After one hour of attachment at 15 ^oC, the inoculum was discarded and fresh ice cold media was added to the cells. Whenever it was necessary to take the samples out of 15 ^oC incubator, they were always kept on ice. Observation by fluorescent microscopy was done three days post-infection. A cooling system was connected to the metal plate that the chamber slide sits on to make sure the low temperature condition was maintained.

Site directed mutagenesis by PCR and subcloning

Mutations were made in a Y420 dsDNA clone using the Polymerase Chain Reaction (PCR) with primers designed to anneal to the flanking regions of the

deleted amino acids. The primers were dissolved in water to 100pmol/μL. 6 μL of this solution was added to 100 μL of water as final solution used for PCR. 6 μL of Y420 plasmid DNA from a large scale prep (Liu and Brown, 1993) was diluted to 100 μL with water and used for PCR. For each mutation, a pair of primers that were complementary to each other were used so that mutations are obtained in both DNA strands. Both strands were mutated in the same PCR reaction using the megaprimer reaction protocol (Sarkar, 1990).

To make sure the PCR reaction and primers do not introduce mutations to other positions in the plasmid DNA, the mutated region was subcloned into the wild type backbone for each mutant strain. To subclone, the region around the deletion was first sequenced to confirm its correctness. That region of the DNA was cut out of the plasmid by selected enzymes. Linear DNA was separated and purified on an agarose gel and cut out under ultraviolet light. Linear DNA with sticky ends was recovered by centrifugation through a filter (DNA gel extraction kit, Millipore Corporation, MA, USA) and ethanol precipitation. The DNA fragment containing the desired mutation was ligated to a healthy Y420 vector that was cut and purified the same way.

Ligation

The two pieces of linear DNA were ligated by fast-link DNA ligation kit from Epicentre Biotechnologies. The molar ratio of the short piece versus the vector was set at 5:1. The total amount of DNA used was about 200ng in 15μl of final reaction

mix. The reaction was done at room temperature overnight. Then the product was transformed into *E.Coli* competent cells (DH5α). Positive colonies were obtained on LB plates containing carbenicillen (80µl/ml) and grown up in 5ml cultures. DNA was extracted by Wizard® Plus Miniprep DNA Purification System from Promega and sequenced. Then a large scale CsCl DNA preparation was done to get concentrated and purified DNA (Liu and Brown, 1993).

Large scale preparation of plasmid DNA

E.coli strain with plasmid DNA was grown from a single colony in 1 L of LB media containing 100µg/ml carbenicillin. Chloramphenicol was added when the culture growth reached log phase. The culture was incubated 20 more hours before being harvested. The cells were spun down and lysed in basic solution. After neutralization and filtration, DNA was precipitated by isopropanol. The sample was then put on a cesium chloride gradient with ethidium bromide, before the DNA band was collected to get rid of RNA. Then ethidium bromide was removed by isopropanol saturated with sodium chloride. The sample was further cleaned by proteinase K treatment and extraction (West et al., 2006).

Transcription, transfection and virus production

Circular double-stranded DNA clones of different virus strains were linearized by XhoI cut and transcribed into positive strand viral RNA by SP6 RNA polymerase. Then viral RNA was transfected into BHK cells by electroporation

Table 5.1: Primer pairs used in PCR reaction to make each mutant.

Mutant	Forward Primer	Reverse Primer
E1Δ433	5'-CTT GCA GCA TGC TGA CTA GCA C-3'	5'-GTG CTA GTC AGC ATG CTG CAA G-3'
E1Δ432-433	5'-GCT TGC AGC CTG ACT AGC ACA C-3'	5'-GTG TGC TAG TCA GGC TGC AAG C-3'
E1Δ422	5'-CTC GTC GCT ATT AAT AGG ACT TAG G-3'	5'-CAT AAG TCC TAT TAA TAG CGA CGA G-3'
E1Δ422-423	5'-GCG GCG CCT CGT CGC TAT TAG GAC TTA TGA TTT TTG CTT G-3'	5'-CAA GCA AAA ATC ATA AGT CCT AAT AGC GAC GAG GCG CCG C-3'
E1Δ420-433	5'-CGC CTC GTC GCT GAC TAG CAC-3'	5'-GTG CTA GTC AGC GAC GAG GCG-3'
E1Δ411-428	5'-TCA AAA ACA TCA TGG AGT TGG CTG GCT TGC AGC ATG ATG CTG ACT AGC-3'	5'-GCT AGT CAG CAT CAT GCT GCA AGC CAG CCA ACT CCA TGA TGT TTT TGA-3'
E1Δ416-433	5'-AGT TGG CTG TTT GCC CTT TTC GGC CTG ACT AGC ACA CGA AGA TGA CCG-3'	5'-CGG TCA TCT TCG TGT GCT AGT CAG GCC GAA AAG GGC AAA CAG CCA ACT-3'
E1Δ413-414	5'-CAT GGA GTT GGC TGT TTG CCG GCG GCG CCT CGT CGC T-3'	5'-AGC GAC GAG GCG CCG CCG GCA AAC AGC CAA CTC CAT G-3'

(Liljestrom and Garoff, 1991). The electroporation was done with a Bio-rad gene pulser at the following settings: 1.5kV of voltage, 25μF of capacitance and ∞ resistance. Cells were allowed to settle down in media afterwards. Virus was collected when CPE was seen, about 24 hours post-transfection. The media containing virus was then harvested and titrated by a plaque assay immediately.

Particle to PFU ratio

10mls of virus was harvested from each transfection. An infection was done immediately upon harvest of the transfection by adding 1ml of virus to each big flask ($75cm^2$). After the inoculum was discarded, 7mls of media was added to each flask. Virus was harvested after CPE was seen, about 18 hours post-infection. Harvested virus was run on a step gradient of tartrate in PBS-D, followed by a continuous gradient (Whitehurst et al., 2006). The virus band was collected from the gradient and subjected to further analysis. After gradient purification, virus was titrated by plaque assay. The same sample of virus was analyzed in a BCA assay to determine protein concentration, with which the concentration of virus particles can be calculated. Particle to PFU ratio was calculated as concentration of virus particles divided by the concentration of PFU as in Whitehurst et al. and Hernandez et al.

Viral protein gel

Viral RNA was produced from in vitro transcription and transfected into BHK cells. Cells were allowed to incubate for 6.5 hours post-transfection (Hernandez et

al., 2000). Actinomycin D was then added to the media to inhibit translation of cellular proteins. The cells are then starved for one hour in methionine-cysteine free medium. After starvation media treatment, [^{35}S] labeled methionine-cysteine mix was added so that radioactive isotopes can be incorporated into viral proteins. After one hour incubation at 37 ^{o}C, the cells are lysed by TNT lysis buffer (1% TritonX-100, 10mM Tris pH7.4, 150mM NaCl, and 0.2 mM phenylmethylsulfonyl fluoride). Viral protein was isolated by polyclonal antibody purified from rabbit serum and conjugated to protein A beads in an immunoprecipitation reaction. After agitation overnight at 5 ^{o}C , viral structural proteins can be spun down with the beads and purified from the mixture. Viral protein can be separated from beads and dissolved in SDS-PAGE loading buffer at pH 6.8. The samples were then run on a denaturing SDS-PAGE gel. The gel was dried and put into a phosphoimager cassette. Exposure was done in the cassette overnight, before the image was read.

Thin sectioning and EM imaging

BHK cell monolayers were fixed with 3% glutaraldehyde (Ladd Research Industries, Inc.) in 0.1M cacodylic acid buffer pH 7.4 (Ladd Research Industries, Inc.) at 4°C. The cells were then washed three times with 0.1 M cacodylic acid and post-fixed with 1% OsO4 in 0.1M cacodylic acid buffer and 0.8% potassium ferricyanide for 30 min. Cells were then washed as before and embedded in 2% agarose. The agarose containing the cell sample was then pre-stained with 1% uranyl acetate (Polaron Instruments, Inc, Hatfield, PA) overnight at 4°C. The

samples were washed and carried through a series of ethanol dehydration steps. Infiltration was done using SPURR compound (LADD Research Industries, Inc.). Sample blocks were trimmed and ultrathin sections were obtained on a LKB NOVA Ultrotome (Leica Microsystems, Inc. Deerfield, IL). Ultrathin sections were then stained with 4% Uranyl acetate in distilled water for 60 min and in Reynolds lead citrate, pH12 (Mallinkdrot Baker Inc. Paris, KY) for 4 min. Samples were observed in a JEOL JEM 100S transmission electron microscope at 80 kV.

CHAPTER 6

References

Bressanelli, S., Stiasny, K., Allison, S. L., Stura, E. A., Duquerroy, S., Lescar, J., Heinz, F. X., and Rey, F. A. (2004). Structure of a flavivirus envelope glycoprotein in its low-pH-induced membrane fusion conformation. *Embo J* **23**(4)**,** 728-38.

Bron, R., Wahlberg, J. M., Garoff, H., and Wilschut, J. (1993). Membrane fusion of Semliki Forest virus in a model system: correlation between fusion kinetics and structural changes in the envelope glycoprotein. *Embo J* **12**(2)**,** 693-701.

Cardoso, R. M., Zwick, M. B., Stanfield, R. L., Kunert, R., Binley, J. M., Katinger, H., Burton, D. R., and Wilson, I. A. (2005). Broadly neutralizing anti-HIV antibody 4E10 recognizes a helical conformation of a highly conserved fusion-associated motif in gp41. *Immunity* **22**(2)**,** 163-73.

Caspar, D. L. D., and Klug, A. (1962). Physical principles in the construction of regular viruses. *Cold Spring Harbor Symp. Quant. Biol.* **27,** 1-24.

Cassell, S., Edwards, J., and Brown, D. T. (1984). Effects of lysosomotropic weak bases on infection of BHK-21 cells by Sindbis virus. *J Virol* **52**(3)**,** 857-64.

Cha, K., Bruel, C., Inglese, J., and Khorana, H. G. (1997). Rhodopsin kinase: expression in baculovirus-infected insect cells, and characterization of post-translational modifications. *Proc Natl Acad Sci U S A* **94**(20)**,** 10577-82.

DeTulleo, L., and Kirchhausen, T. (1998). The clathrin endocytic pathway in viral infection. *Embo J* **17**(16)**,** 4585-93.

Eckert, D. M., and Kim, P. S. (2001). Mechanisms of viral membrane fusion and its inhibition. *Annu Rev Biochem* **70,** 777-810.

Edwards, J., and Brown, D. T. (1986). Sindbis virus-mediated cell fusion from without is a two-step event. *J Gen Virol* **67**(Pt 2)**,** 377-80.

Ford T., G. J., Rickwood D. (1994). Iodixanol: A Nonionic Iso-osmotic Centrifugation Medium for the Formation of Self-Generated Gradients *Analytical Biochemistry* **220**(2)**,** 360-366.

Fuller, S. D. (1987). The T=4 envelope of Sindbis virus is organized by interactions with a complementary T=3 capsid. *Cell* **48**(6)**,** 923-34.

Gaedigk-Nitschko, K., and Schlesinger, M. J. (1990). The Sindbis virus 6K protein can be detected in virions and is acylated with fatty acids. *Virology* **175**(1)**,** 274-81.

Gibbons, D. L., Vaney, M. C., Roussel, A., Vigouroux, A., Reilly, B., Lepault, J., Kielian, M., and Rey, F. A. (2004). Conformational change and protein-protein interactions of the fusion protein of Semliki Forest virus. *Nature* **427**(6972)**,** 320-5.

Haywood, A. M., and Boyer, B. P. (1985). Fusion of influenza virus membranes with liposomes at pH 7.5. *Proceedings of the National Academy of Science* **82,** 4611-4615.

Helenius, A. (1984). Semliki Forest virus penetration from endosomes: a morphological study. *Biol Cell* **51**(2)**,** 181-5.

Helenius, A., and Marsh, M. (1982). Endocytosis of enveloped animal viruses. *Ciba Found Symp* **92,** 59-76.

Helenius, A., Marsh, M., and White, J. (1982). Inhibition of Semliki forest virus penetration by lysosomotropic weak bases. *J Gen Virol* **58 Pt 1,** 47-61.

Hernandez, R., Lee, H., Nelson, C., and Brown, D. T. (2000). A single deletion in the membrane-proximal region of the Sindbis virus glycoprotein E2 endodomain blocks virus assembly. *J Virol* **74**(9)**,** 4220-8.

Hernandez, R., Luo, T., and Brown, D. T. (2001). Exposure to low pH is not required for penetration of mosquito cells by Sindbis virus. *J Virol* **75**(4)**,** 2010-3.

Hernandez, R., Sinodis, C., Horton, M., Ferreira, D., Yang, C., and Brown, D. T. (2003). Deletions in the transmembrane domain of a sindbis virus glycoprotein alter virus infectivity, stability, and host range. *J Virol* **77**(23)**,** 12710-9.

Hernandez, R. e. a. (2006). Sindbis virus: Propagation, Quantification and Storage. *In* "Current Protocols in Microbiology" (R. e. a. Coico, Ed.), Vol. 1, pp. 15B.1. John Wiley and Sons.

Jardetzky, T. S., and Lamb, R. A. (2004). Virology: a class act. *Nature* **427**(6972)**,** 307-8.

Kielian, M. (1995). Membrane fusion and the alphavirus life cycle. *Adv Virus Res* **45,** 113-51.

Kielian, M., Chatterjee, P. K., Gibbons, D. L., and Lu, Y. E. (2000). Specific roles for lipids in virus fusion and exit. Examples from the alphaviruses. *Subcell Biochem* **34,** 409-55.

Kielian, M., and Jungerwirth, S. (1990). Mechanisms of enveloped virus entry into cells. *Mol Biol Med* **7**(1)**,** 17-31.

Kielian, M. C., and Helenius, A. (1984). Role of cholesterol in fusion of Semliki Forest virus with membranes. *J Virol* **52**(1)**,** 281-3.

Kim, H., Lee, S. J., Park, J. Y., Park, Y. W., Kim, H. S., Kang, H. Y., Hur, B. K., Ryu, Y. W., Han, S. I., and Kim, J. S. (2004). Study on persistent infection of Japanese

encephalitis virus Beijing-1 strain in serum-free Sf9 cell cultures. *J Microbiol* **42**(1)**,** 25-31.

Koschinski, A., Wengler, G., Wengler, G., and Repp, H. (2005). Rare earth ions block the ion pores generated by the class II fusion proteins of alphaviruses and allow analysis of the biological functions of these pores. *J Gen Virol* **86**(Pt 12)**,** 3311-20.

Liljestrom, P., and Garoff, H. (1991). Internally located cleavable signal sequences direct the formation of Semliki Forest virus membrane proteins from a polyprotein precursor. *J Virol* **65**(1)**,** 147-54.

Liljestrom, P., Lusa, S., Huylebroeck, D., and Garoff, H. (1991). In vitro mutagenesis of a full-length cDNA clone of Semliki Forest virus: the small 6,000-molecular-weight membrane protein modulates virus release. *J. Virol.* **65,** 4107-4113.

Lippincott-Schwartz, J., Roberts, T. H., and Hirschberg, K. (2000). Secretory protein trafficking and organelle dynamics in living cells. *Annu Rev Cell Dev Biol* **16,** 557-89.

Liu, N., and Brown, D. T. (1993). Transient translocation of the cytoplasmic (endo) domain of a type I membrane glycoprotein into cellular membranes. *J Cell Biol* **120**(4)**,** 877-83.

Long, F., Wang, Y. X., Liu, L., Zhou, J., Cui, R. Y., and Jiang, C. L. (2005). Rapid nongenomic inhibitory effects of glucocorticoids on phagocytosis and superoxide anion production by macrophages. *Steroids* **70**(1)**,** 55-61.

Lopez, S., Yao, J. S., Kuhn, R. J., Strauss, E. G., and Strauss, J. H. (1994). Nucleocapsid-glycoprotein interactions required for assembly of alphaviruses. *J Virol* **68**(3)**,** 1316-23.

Lu, Y. E., Cassese, T., and Kielian, M. (1999). The cholesterol requirement for sindbis virus entry and exit and characterization of a spike protein region involved in cholesterol dependence. *J Virol* **73**(5)**,** 4272-8.

Lu, Y. E., and Kielian, M. (2000). Semliki forest virus budding: assay, mechanisms, and cholesterol requirement. *J Virol* **74**(17)**,** 7708-19.

Lusa, S., Garoff, H., and Liljestrom, P. (1991). Fate of the 6K membrane protein of Semliki forest virus during virus assembly. *Virology* **185,** 843-846.

Luukkonen, A., Brummer-Korvenkontio, M., and Renkonen, O. (1973). Lipids of cultured mosquito cells (Aedes albopictus). Comparison with cultured mammalian fibroblasts (BHK 21 cells). *Biochim Biophys Acta* **326**(2)**,** 256-61.

Marsh, M., Bolzau, E., and Helenius, A. (1983). Penetration of Semliki Forest virus from acidic prelysosomal vacuoles. *Cell* **32**(3)**,** 931-40.

Marsh, M., and Helenius, A. (2006). Virus entry: open sesame. *Cell* **124**(4)**,** 729-40.

Marsh, M., Helenius, Ari. (2006). Virus Entry: Open Sesame. *Cell* **124**(4)**,** 729-740.

Moehring, J. M., Inocencio, N. M., Robertson, B. J., and Moehring, T. J. (1993). Expression of mouse furin in a Chinese hamster cell resistant to Pseudomonas exotoxin A and viruses complements the genetic lesion. *J Biol Chem* **268**(4)**,** 2590-4.

Mulvey, M., and Brown, D. T. (1994). Formation and rearrangement of disulfide bonds during maturation of the Sindbis virus E1 glycoprotein. *J Virol* **68**(2)**,** 805-12.

Paredes, A. M., Brown, D. T., Rothnagel, R., Chiu, W., Schoepp, R. J., Johnston, R. E., and Prasad, B. V. (1993). Three-dimensional structure of a membrane-containing virus. *Proc Natl Acad Sci U S A* **90**(19)**,** 9095-9.

Paredes, A. M., Ferreira, D., Horton, M., Saad, A., Tsuruta, H., Johnston, R., Klimstra, W., Ryman, K., Hernandez, R., Chiu, W., and Brown, D. T. (2004). Conformational changes in Sindbis virions resulting from exposure to low pH and interactions with cells suggest that cell penetration may occur at the cell surface in the absence of membrane fusion. *Virology* **324**(2)**,** 373-86.

Renz, D., and Brown, D. T. (1976). Characteristics of Sindbis virus temperature-sensitive mutants in cultured BHK-21 and Aedes albopictus (Mosquito) cells. *J Virol* **19**(3)**,** 775-81.

Rietveld, A., Neutz, S., Simons, K., and Eaton, S. (1999). Association of sterol- and glycosylphosphatidylinositol-linked proteins with Drosophila raft lipid microdomains. *J Biol Chem* **274**(17)**,** 12049-54.

Rietveld, A. G., Koorengevel, M. C., and de Kruijff, B. (1995). Non-bilayer lipids are required for efficient protein transport across the plasma membrane of Escherichia coli. *Embo J* **14**(22)**,** 5506-13.

Sarkar, G. S., S.S. (1990). The "megaprimer " method of site directed mutagenesis. *BioTechniques* **8,** 404-407.

Smit, J. M., Li, G., Schoen, P., Corver, J., Bittman, R., Lin, K. C., and Wilschut, J. (2002). Fusion of alphaviruses with liposomes is a non-leaky process. *FEBS Lett* **521**(1-3)**,** 62-6.

Stegmann, T., Booy, F. P., and Wilschut, J. (1987). Effects of low pH on influenza virus. Activation and inactivation of the membrane fusion capacity of the hemagglutinin. *J Biol Chem* **262**(36)**,** 17744-9.

Stegmann, T., Hoekstra, D., Scherphof, G., and Wilschut, J. (1985). Kinetics of pH-dependent fusion between influenza virus and liposomes. *Biochemistry* **24**(13)**,** 3107-13.

Strauss, E. G., Lenches, E. M., and Strauss, J. H. (2002). Molecular genetic evidence that the hydrophobic anchors of glycoproteins E2 and E1 interact during assembly of alphaviruses. *J Virol* **76**(20)**,** 10188-94.

Strauss, E. G., Rice, C. M., and Strauss, J. H. (1983). Sequence coding for the alphavirus nonstructural proteins is interrupted by an opal termination codon. *Proc Natl Acad Sci U S A* **80**(17)**,** 5271-5.

Strauss, J. H., and Strauss, E. G. (1994). The Alphaviruses: Gene Expression, Replication, and Evolution. Micro. Rev. 58:491-562. *Micro. Rev* **58,** 491-562.

Tamm, L. K. (2003). Hypothesis: spring-loaded boomerang mechanism of influenza hemagglutinin-mediated membrane fusion. *Biochim Biophys Acta* **1614**(1)**,** 14-23.

Ulug, E. T., Garry, R. F., Waite, M. R., and Bose, H. R., Jr. (1984). Alterations in monovalent cation transport in Sindbis virus-infected chick cells. *Virology* **132**(1)**,** 118-30.

Vogel, R. H., Provencher, S. W., von Bonsdorff, C. H., Adrian, M., and Dubochet, J. (1986). Envelope structure of Semliki Forest virus reconstructed from cryo-electron micrographs. *Nature* **320**(6062)**,** 533-5.

von Bonsdorff, C. H., and Harrison, S. C. (1975). Sindbis virus glycoproteins form a regular icosahedral surface lattice. *J. Virol.* **16**(1)**,** 141-5.

Weeks, B. A., Keisler, A. S., Myrvik, Q. N., and Warinner, J. E. (1987). Differential uptake of neutral red by macrophages from three species of estuarine fish. *Dev Comp Immunol* **11**(1)**,** 117-24.

Weiss, B., Nitschko, H., Ghattas, I., Wright, R., and Schlesinger, S. (1989). Evidence for specificity in the encapsidation of Sindbis virus RNAs. *J Virol* **63**(12)**,** 5310-8.

Weiss, S. A., Godwin, G. P., Gorfien, S. F., and Whitford, W. G. (1993). Insect cell culture engineering. Serum-free media. *Bioprocess Technol* **17,** 179-94.

West, J., Hernandez, R., Ferreira, D., and Brown, D. T. (2006). Mutations in the endodomain of Sindbis virus glycoprotein E2 define sequences critical for virus assembly. *J Virol* **80**(9)**,** 4458-68.

White, J., Kartenbeck, J., and Helenius, A. (1980). Fusion of Semliki Forest Virus with the plasma membrane can be induced by low pH. *Journal of Cell Biology* **87,** 264-272.

Whitehurst, C. B., Soderblom, E. J., West, M. L., Hernandez, R., Goshe, M. B., and Brown, D. T. (2007). Location and role of free cysteinyl residues in the Sindbis virus E1 and E2 glycoproteins. *J. Virol.* **81**(12)**,** 6231-40.

Whitehurst, C. B., Willis, J. H., Sinodis, C. N., Hernandez, R., and Brown, D. T. (2006). Single and multiple deletions in the transmembrane domain of the Sindbis virus E2 glycoprotein identify a region critical for normal virus growth. *Virology* **347**(1)**,** 199-207.